On the application of photocatalyst-sorbent composite materials for arsenic(III) remediation: insights from kinetic adsorption modelling

[1*]Jay C. Bullen; [2,3]Chaipat Lapinee; [4]Pascal Salaün; [3]Ramon Vilar and [1*]Dominik J. Weiss

[1]Department of Earth Science and Engineering, Imperial College London, London SW7 2AZ, United Kingdom

[2]Department of Chemistry, School of Science, University of Phayao, Phayao 56000, Thailand

[3]Department of Chemistry, Imperial College London, White City Campus, London W12 OBZ, United Kingdom

[4]School of Environmental Sciences, University of Liverpool, Liverpool L69 3GP, United Kingdom

*Corresponding authors:

Email: j.bullen16@imperial.ac.uk; d.weiss@imperial.ac.uk

Graphical abstract

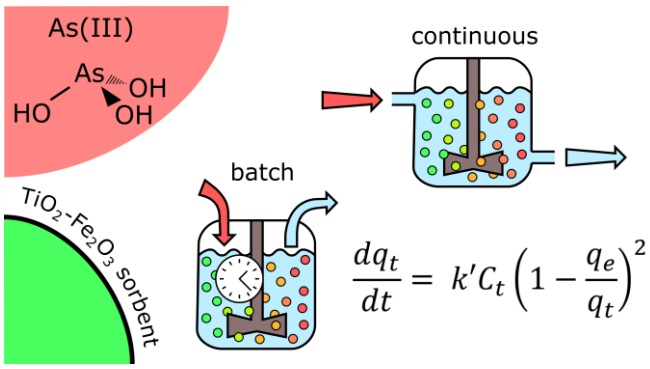

Keywords

Batch; continuous-flow; arsenic remediation; remediation; pseudo-second order; adsorption kinetics

Abstract

TiO_2-Fe_2O_3 composites show great promise for the removal of arsenic(III) from drinking water: this single material combines the photocatalytic capabilities of TiO_2 for the oxidation of arsenite (i.e. As(III)) with the high adsorption capacity of Fe_2O_3 towards the arsenate (i.e. As(V)) subsequently produced. To design an effective treatment, it is necessary to balance high sorbent concentrations, providing long filter lifetimes, with low photocatalyst concentrations, to achieve effective penetration of light into the system. In this work, we construct a predictive model using experimentally determined As(III) adsorption isotherms and kinetics to estimate arsenic treatment plant lifetimes. We considered sorbent loading, treatment time, and batch treatment versus continuous-flow. Our model indicated that batch treatment is more efficient than continuous-flow at low sorbent concentrations (<100 g L^{-1}), and therefore more appropriate for the photocatalyst-sorbent system. However, with <100 g L^{-1} sorbent, media should be replaced several times per year to maintain effective treatment. In contrast, slurries of >100 g L^{-1} sorbent could operate for an entire year without media replacement. This work highlights

the important implications of sorbent concentration when we consider the multifunctional photocatalysts-sorbent system, and highlights the need for further experimental work to design efficient arsenic treatment plants.

1. Introduction

The arsenic treatment plants developed for South Asia often fail to provide safe drinking water [1]. One study of 200 plants in rural Uttar Pradesh, India, found that after 10 years only 34 were still in operation, of which only one plant delivered water below the 10 μg L^{-1} WHO safety limit [1]: the remaining 97% of treatment plants were providing unsafe water. Much of the difficulty in providing safe water in South Asia lies in the anoxic, reducing groundwater conditions, where arsenic is found in the +3 oxidation state, i.e. neutral H_3AsO_3, which adsorbs weakly to sorbent media. Pre-oxidation of arsenite, As(III), to more strongly adsorbing, negatively charged arsenate, As(V), oxyanions (i.e. $H_2AsO_4^-$ and $HAsO_4^{2-}$ at neutral pH) is thus important for effective removal [2]. Whilst oxidation of As(III) can be achieved through application of conventional chemical oxidants such as chlorine, permanganate, ozone, and Fenton's reagent [3] [4], limitations include the risk of toxic disinfection by-products (DBPs) such as carcinogenic trihalomethanes (particularly relevant in South Asia due to the high levels of dissolved organic matter present in arsenic-contaminated groundwaters) [4] [5]. Oxidation using heterogeneous photocatalysts such as TiO_2 reduces the risk of DBPs [6], and mixed mineral oxide composites such as TiO_2-Fe_2O_3 are especially attractive, as they combine photocatalytic oxidation of As(III) to As(V), using the TiO_2 phase, with effective adsorption of As(V) to the Fe_2O_3 phase [7] [8] [9].

To date, however, photocatalyst-sorbent materials remain untested for real-life applications in As(III) remediation. An important yet unanswered question when engineering the photocatalyst-sorbent system is how much material should be used. Low concentrations of suspended photocatalysts (<1 g L^{-1}) are typical for As(III) photooxidation, to achieve effective light penetration through the system [10] [11] [11] [12] [13] [14]. Whilst linear relationships between TiO_2 concentrations and reaction rates are often observed at low catalyst concentrations, at high catalyst concentrations reaction rates become limited by the supply of photons and by light scattering effects [12]. Reaction rates may even decrease with excess photocatalyst concentrations [15]. However, low sorbent concentrations lead to low adsorption capacities and limited filter life-times, after which saturated sorbent media (i.e. with no adsorption capacity remaining) must be replaced or regenerated. Sorbent life-time is a major factor determining the success or failure of arsenic mitigation schemes in South Asia: users often fail to replace or

regenerate saturated sorbent media due to lack of expertise [16] or lack of confidence [17]. A recent study of three arsenic mitigation microenterprises across India and Bangladesh found that robustness and reliability of the sorbent material was the most important technological factor for sustaining and growing these schemes [18].

Another limitation to sustaining arsenic remediation programs is the cost of replacement sorbent media [16]. Improving economic efficiency requires maximising the concentration of arsenic loaded on the sorbent before breakthrough (breakthrough is where the material is saturated, and arsenic emerges in the effluent). Factors affecting sorbent economy include not just the amount of sorbent used, but also how it is used, e.g. the choice between batch and continuous-flow treatments [19]. In a batch treatment, discrete volumes of water are treated sequentially, for a designated time, after which the effluent hopefully meets safety guidelines. In a continuous-flow treatment, influent and effluent are continuously pumped into and out of the reactor, and flow-rate becomes another consideration. Sorbent economy is improved with slow flow rates, but users of household arsenic filtration systems have previously complained that the flow-rates of current products are too slow [17].

The efficiency of different treatment designs can be defined both by their sorbent economy, and the volume of water treated before effluent exceeds the maximum contaminant level (MCL). Most household and community-scale solutions for the treatment of arsenic-contaminated water use sorbent media in a continuous-flow, column arrangement [1] [20]. It is commonly believed that continuous-flow adsorption is more efficient than batch treatment, but under certain conditions batch treatment can prove superior [19], and despite many studies on novel sorbents conducting both batch and column experiments, few papers provide a comparison between the merits of each treatment. In the field of environmental remediation, photocatalysts are also deployed in both batch and continuous-flow devices [21]. Photocatalytic performance can vary between the two processes, e.g. one study found that photocatalytic degradation of dyes was up to 110% more effective under continuous-flow treatment [15]. It is non-trivial to compare the efficiency of batch and continuous-flow treatments, for instance batch treatments are defined by the time required (minutes per unit volume) whilst continuous-flow is

defined by the rate (volume per minute) and bed volumes treated before breakthrough, and subsequently the lack of substantive cross-evaluation is not surprising [22].

Previous work on the relative merits of batch and continuous-flow design includes the study of Dichiara et al., where a 'critical concentration' parameter was calculated from experimentally determined coefficients (pertaining to the fixed bed sorbate removal efficiency, and incorporating effects such as pore channelling) [19]. When the target effluent concentration (e.g. the MCL) exceeds this critical concentration, batch treatment gives a better sorbent economy than fixed bed column treatments, and vice versa. Lekić et al. compared the efficiencies of their sorbent (iron-manganese oxide coated sand) for As(III) and As(V) removal in batch and column configurations by comparing the amount of arsenic removed per gram of sorbent [23]. They found that continuous-flow columns were more efficient than batch treatment, which they suggested was due to non-adsorption processes such as coagulation, flocculation and filtration [23].

The risk of exposure to arsenic contaminated water in South Asia is greatest amongst the rural poor [24] [25]. Rural communities often lack access to replacement parts and expertise in maintaining filter systems, two major reasons for the short-lifetimes of arsenic mitigation schemes [16]. Electrical outages [26] and the challenge of maintaining equipment [17] mean that a system based on photooxidation-sorbent needs a fail-safe option, i.e. the device should provide reasonable removal of As(III) in the absence of photooxidation.

The aim of this work was to determine the minimum concentration of TiO_2-Fe_2O_3 needed for an arsenic treatment plant, considering the worst-case scenario that the material is operated as a sorbent only. To achieve this aim, our objectives were: (1) to experimentally determine adsorption isotherms and kinetics as input parameters for simulating the As(III)/TiO_2-Fe_2O_3 system; (2) to develop a kinetic model capable of describing As(III) adsorption that is sensitive to changes in both sorbent and sorbate concentration; (3) to investigate the influence of sorbent concentration on batch and continuous-flow treatments; (4) to investigate sorbent life-times in both systems, simulating a single household's clean

water requirement over a 365-day period; and finally (5) to recommend a reactor design for use in subsequent experimental work.

2. Experimental

2.1. Synthesis of a TiO_2-Fe_2O_3 bi-functional sorbent

The synthesis of a TiO_2-Fe_2O_3 bi-functional sorbent was carried out in two steps, by small modifications of a previously reported procedure [27] [7]. Firstly, mesoporous anatase TiO_2 was produced via sol-gel synthesis [28]. For this, pluronic P123 (1 g, Aldrich) was dissolved in absolute ethanol (12 g, VWR, ACS Puriss grade), and $Ti(OBu^n)_4$ (2.7 g, ACROS Organics, 99% purity) was dissolved in concentrated HCl (3.2g, ACROS Organics, ACS reagent grade, ca. 37%). The P123 solution was then added dropwise to the solution of $Ti(OBu^n)_4$ and the mixture was aged at room temperature with continuous stirring, until a gel-like white film of TiO_2 was formed. The product was calcined at 350 °C for 4 hours (temperature ramped at 1 $^oC\ min^{-1}$), cooled to room temperature, and then crushed. In the second step, this mesoporous TiO_2 (1.5 g) was added to an ethanolic solution of 0.6 M $Fe(NO_3)_3 \cdot 9H_2O$ (48.5 g, Sigma-Aldrich, ACS reagent grade, >98%). The mixture was stirred for 30 min, then heated at 50 ^oC to evaporate the solvent. The product was calcined in a furnace at 300 °C for 10 min, then cooled and crushed. The product was calcined a final time, at 300 °C for 6 hours. The material was ground to a homogeneous powder and stored in a desiccator. The theoretical TiO_2:Fe_2O_3 mass ratio was 1:1, based on the quantities of reagents used. TiO_2-Fe_2O_3 was characterised using XRD and SEM, and the BET-specific surface area, surface charge, and zeta potential were determined, as discussed in the Supplementary Information.

2.2. Determination of adsorption capacity and kinetic parameters

Adsorption isotherms and kinetic parameters for the arsenic treatment plant model were obtained, with the experimental procedure described in the Supplementary Information. Briefly, adsorption isotherms were determined, and then modelled using the Langmuir and Freundlich equations [29]. Adsorption kinetics were determined, and then modelled using the pseudo-first and pseudo-second order rate equations [30]. As(III) concentrations were determined electrochemically by Anodic Stripping

Voltammetry (ASV) [31] [32] [33]. Experiments were carried out in triplicate and uncertainties calculated as the standard deviation between results. For adsorption isotherm parameters, uncertainties were propagated from the standard error in the slope and y-intercept of the linearised plots. For pseudo-second order kinetic parameters, uncertainties were determined using the Monte Carlo nonlinear regression method reported by Hu et al. [34].

2.3. Predictive modelling of adsorption kinetics

The kinetic adsorption model aimed to investigate As(III) removal under different initial sorbate (C_0) and sorbent (C_s) concentrations. A demonstration of how the pseudo-second order (PSO) model can be modified to provide better sensitivity towards changes in C_0 and C_s is given elsewhere [35], with a modified rate equation that takes the form:

$$\frac{dq_t}{dt} = k' C_t \left(1 - \frac{q_e}{q_t}\right)^2$$

Equation 1

where t is time (minutes), q_t and q_e are the concentrations of As(III) adsorbed at time t and at equilibrium, respectively (mg g^{-1}), k' is the rate constant (L g^{-1} min^{-1}), C_t is the concentration of aqueous As(III) at time t, and k' is derived from PSO parameters via:

$$\mathrm{k}' = \frac{k_2 {q_e}^{\dagger 2}}{{C_0}^{\dagger}}$$

Equation 2

where k_2 is the PSO rate constant (g mg^{-1} min^{-1}), and ${q_e}^{\dagger 2}$ (mg g^{-1}) and ${C_0}^{\dagger}$ (mg L^{-1}) denote the values of q_e and C_0 under the original experimental conditions [35]. The expression for second-order dependence upon the relative amount of available adsorption capacity remaining, $\left(1 - \frac{q_e}{q_t}\right)^2$, is the same expression seen elsewhere, such as the integrated kinetic Langmuir model [36]. In this modified kinetic model, q_e

was calculated at each point in time using the experimentally determined Freundlich adsorption isotherm, given by:

$$q_e = K_F C_e^{1/n}$$

Equation 3

where C_e is the concentration of aqueous sorbate at equilibrium (mg L^{-1}), and the Freundlich constant, K_F (mg g^{-1} (mg L^{-1}) $^{-1/n}$) and n (unitless) are experimentally determined constants [29]. It has been shown that using adsorption isotherms to calculate the PSO parameter q_e outside of equilibrium, at each point in time, gives a better account of initial adsorption kinetics than when using the fixed value of q_e calculated from the linearised PSO kinetics [37].

2.4. Continuous-flow model

The continuous flow reactor design was modelled by adding terms to Equation 1 that account for the influx and outflux of As(III) with continuous pumping:

$$\frac{dC_t}{dt} = jC_{influent} - C_s k' C_t \left(1 - \frac{q_e}{q_t}\right)^2 - jC_t$$

Equation 4

where j is the reactor turnover rate (min^{-1}), indicating the time taken to produce one bed volume of effluent, and $C_{influent}$ is the concentration of influent As(III) (mg L^{-1}). $jC_{influent}$ reflects the increase in C_t due to influx of the influent, whilst jC_t represents As(III) lost via the effluent.

Continuous flow reactors were modelled with C_s varied between 0.01 and 10 000 g L^{-1} and C_0 was set at 0.5, 1, or 2 mg L^{-1}. The parameter j was varied between 0.001 and 1 min^{-1} to reflect reactor residence times (i.e. treatment times) between one minute and one day.

2.5. Modelling 365 days of treatment

To model 365 days of sequential batch treatments using the same mass of sorbent, we considered a reactor operated once per day on a single volume of water, as per Colombo and Ashokkumar [15]. 365 consecutive simulations were conducted, each representing a single day: in each simulation the initial value of q_t was set equal to the final value of q_t in the previous simulation, to reflect increasing saturation of the sorbent with each passing day. The size of the reactor was set as 40 L household^{-1} to meet clean water requirements, and the quantity of sorbent needed per household calculated as $mass\ of\ sorbent\ (g\ household^{-1}) = V\ (40\ L\ household^{-1}) \cdot C_s\ (g\ L^{-1})$.

To model the continuous-flow system, (a) the number of bed volumes successfully treated in 365 days ($BV\ (year^{-1}) = j\ (min^{-1}) \cdot 525\ 600\ (\min year^{-1})$) and (b) the number of bed volumes treated before breakthrough were both determined, and the lesser of the two was used as a measure of the volume of safe water produced in 365 days. The size of the reactor was calculated as the minimum size required to provide 40 L^{-1} household^{-1} day^{-1}, using the equation $V\ (L) =\ 40\ (L\ household^{-1}\ day^{-1}) \cdot j(min^{-1}) \cdot 1440\ (\min day^{-1})$. In both systems, sorbent efficiency was determined as the concentration of As(III) either (a) adsorbed at breakthrough, or (b) after 365 days (whichever came sooner). The 'average residence time' (min) was calculated as the inverse of turnover rate.

2.6. Simulations using MATLAB

Differential equations (Equation 1 and Equation 4) were solved using custom-built MATLAB codes, provided in the Supplementary Information [38].

For each simulation, the input parameters were C_0, C_s, $C_{influent}$, j, k', K_F, n and q_0 (where q_0 is the initial concentration of adsorbed As(III), being only non-zero when simulating 365 days of batch treatment). The end-point of each simulation was set as 1440 minutes for the batch system, and calculated as a product of $C_{influent}$ and j^{-1} for the continuous-flow system. 2000 data points were calculated, with shorter time intervals during the initial stages of reaction (where C_t and q_t are fastest to change), giving better resolution. The differential equations were solved using ODE15s or ODE45 functions and the output saved to a .txt file.

For both systems As(III) concentrations of 500 and 2000 μg L^{-1} were considered, representing the most severe arsenic contamination observed in South Asia [39]. The system was simplified by not including phosphate and sulphate anions which would compete with arsenic for sorbent binding sites. K_F was rescaled to better fit the kinetic data, owing to an increase in the adsorption of As(III) at C_e=23 mg L^{-1} observed in the kinetic experiment compared with the adsorption isotherm.

3. Results and discussion

3.1. Determining parameters for modelling adsorption capacity

Understanding adsorption capacity and adsorption mechanisms is essential for developing kinetic adsorption models. As(III) adsorption isotherms at pH 5, 7 and 9 were determined and modelled using the Langmuir and Freundlich adsorption isotherms (Figure 1). Isotherm parameters are presented in

Table 1. On average, the Freundlich adsorption isotherm model gave a better fit (R^2=0.7996±0.0786) than the Langmuir model (R^2=0.7583±0.0347), however results were within error of one another.

Previous studies have also fit As(III) adsorption to TiO_2 and Fe_2O_3 using both isotherm models. Examples of Freundlich behaviour at circumneutral pH include Gupta et al. (TiO_2) [40] and Tang et al. (Fe_2O_3) [41]. Examples of Langmuir-type behaviour at circumneutral pH include Pan and Hu (TiO_2) [42] and Giménez (Fe_2O_3) [43]. Dutta et al. found a superior fit with the Freundlich adsorption isotherm for As(III) adsorption over TiO_2 at both pH 4 and 9 [44]. Deedar et al. found that As(III) adsorption over TiO_2 was best described by the Langmuir adsorption isotherm, however it is unclear whether the difference was statistically significant [45]. In this work, As(III) adsorption capacities were higher than the previously reported capacities for As(V) adsorption over TiO_2-Fe_2O_3 with 12.14±0.42, 7.79±0.20 and 6.48±0.30 mg g^{-1}, at pH 5, 7 and 9 respectively [27]. This is potentially due to multilayer adsorption of As(III), which has been identified in several studies [46]. The Freundlich adsorption model was subsequently used throughout the rest of this work.

Maximum adsorption of As(III) occurred at pH 5 (Figure 1). Previous studies of composite photocatalyst-sorbents include γ-Fe_2O_3@ZrO_2, which showed maximum As(III) adsorption at pH 8-9 [47], and iron-doped TiO_2, with a maximum at pH 7 [45]. As(III) adsorption to TiO_2 typically shows a maximum at alkaline pH values: at pH 8 [42], pH 9 [40] or pH 8-10 [48], whilst As(III) demonstrates maximum adsorption to iron oxides at lower pH, for instance pH 6 for Fe_2O_3 [49]. The γ-Fe_2O_3 nanosheets of Liu et al. showed increasing As(III) adsorption with increasing acidity, down to pH 3 [50]. The increased adsorption of As(III) at pH 5 suggests that adsorption to our TiO_2-Fe_2O_3 composite is primarily controlled by the Fe_2O_3 phase, rather than by TiO_2.

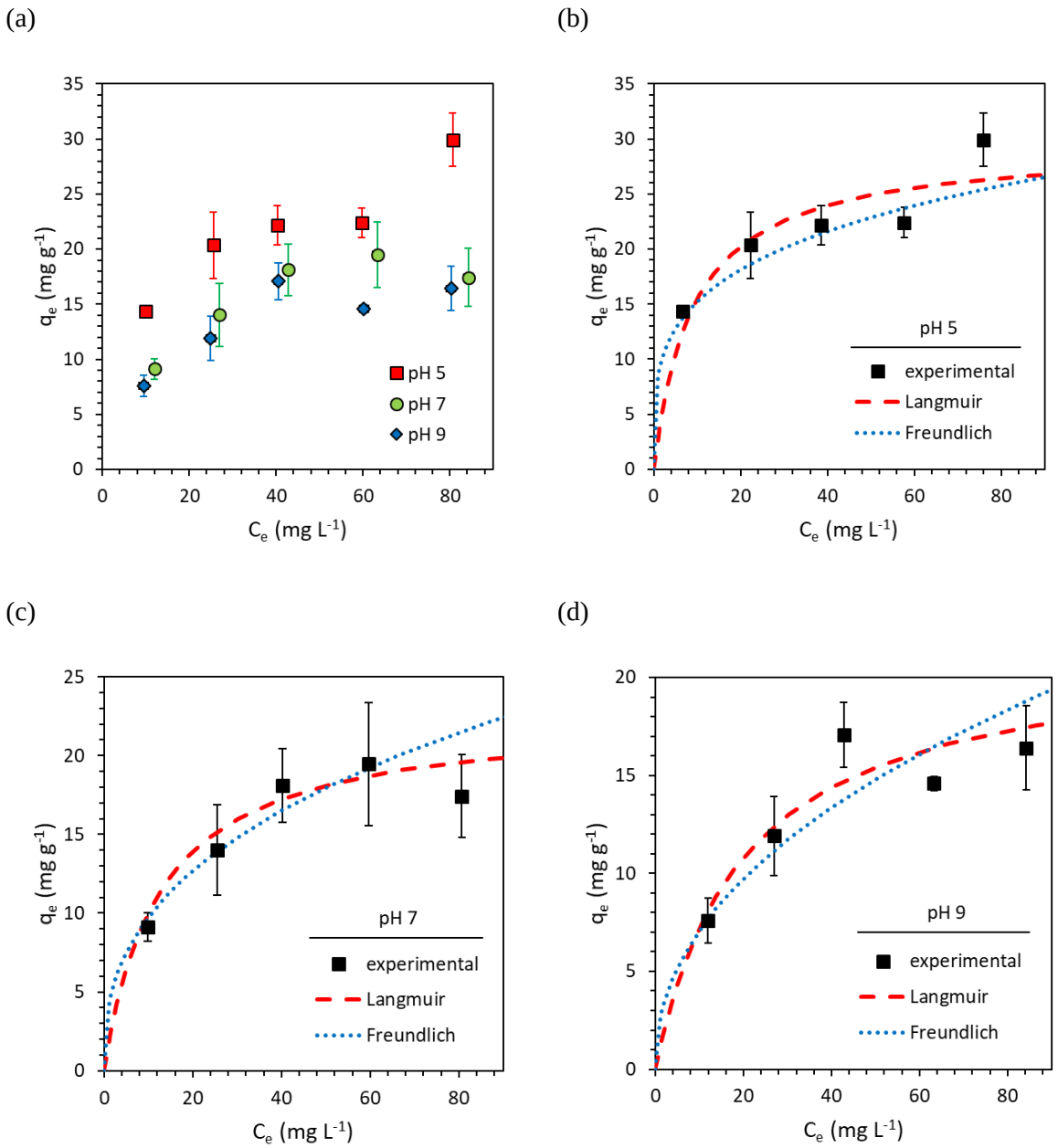

Figure 1: As(III) adsorption isotherms using the TiO_2-Fe_2O_3 multifunctional sorbent. The influence of pH on adsorption isotherms is presented in (a), and a comparison of Langmuir and Freundlich adsorption isotherms is made at (b) pH 5, (c) pH 7, and (d) pH 9. Experimental conditions were 20-100 mg L^{-1} total As(III), 1 g L^{-1} sorbent, and buffered electrolytes: either 0.01 M acetate (pH 5), 0.01 M HEPES (pH 7), or 0.01 M borate (pH 9). Error bars show the standard deviation between three repeat experiments.

Table 1: Langmuir and Freundlich parameters for As(III) adsorption onto TiO_2-Fe_2O_3. R^2 is the coefficient of determination, representing the goodness of fit between experiment and model in the non-linear adsorption isotherm. For the linear equations, R^2 values were 0.93, 0.97 and 0.94 for Langmuir adsorption isotherms at pH 5, 7 and 9 respectively, and 0.78, 0.88 and 0.84 for Freundlich adsorption isotherms at pH 5, 7 and 9 respectively. Uncertainties were propagated using the standard deviation of the slope and y-intercept parameters of the linear regression. The BET-specific surface area of TiO_2-Fe_2O_3 was 63.1 m^2 g^{-1}.

pH	Langmuir parameters					Freundlich parameters		
	Q_{max}			K_L	R^2	K_F	n	R^2
	(mg g^{-1})	(mg m^{-2})	(μmol m^{-2})	(L mg^{-1})		(mg g^{-1} (mg L^{-1})$^{-1/n}$)	(unitless)	
5	29.44 ±2.99	0.47±0.05	6.21±0.66	0.11±0.07	0.7219	8.47±2.64	3.94±0.95	0.8835
7	22.64±1.74	0.36±0.03	4.81±0.37	0.08±0.03	0.7909	4.06±1.15	2.63±0.14	0.7874
9	21.60±0.33	0.35±0.01	4.61±0.09	0.05±0.01	0.7622	2.46±0.75	2.18±0.25	0.7278

3.2. Determining parameters for modelling adsorption kinetics

Understanding the kinetics of As(III) adsorption is essential for determining appropriate flow rates and treatment times, if multifunctional sorbents are to be incorporated into an arsenic treatment plant. To this end, we tested both pseudo-first order (PFO) and pseudo-second order (PSO) kinetic models, and obtained conditional rate constants.

As(III) concentrations decreased very fast within the first 5 minutes of mixing and reached equilibrium within approximately 25 minutes (Figure 2). Slower As(III) adsorption kinetics have been observed on other composite photocatalyst-sorbents, with equilibrium reached in 180 minutes for γ-Fe_2O_3-TiO_2 (C_0=1 mg L^{-1}, C_s=0.5 g L^{-1}, pH 7.0) [8] and 120 minutes for γ-Fe_2O_3@ZrO_2 (C_0=100 mg L^{-1}, C_s=1 g L^{-1}, pH 9) [47]. However, Li et al. found that Pb(II) adsorption over Fe_2O_3-TiO_2 composite materials reached equilibrium very rapidly, in just 5 minutes (C_0 = 10-80 mg L^{-1}, C_s=1 g L^{-1}) [51].

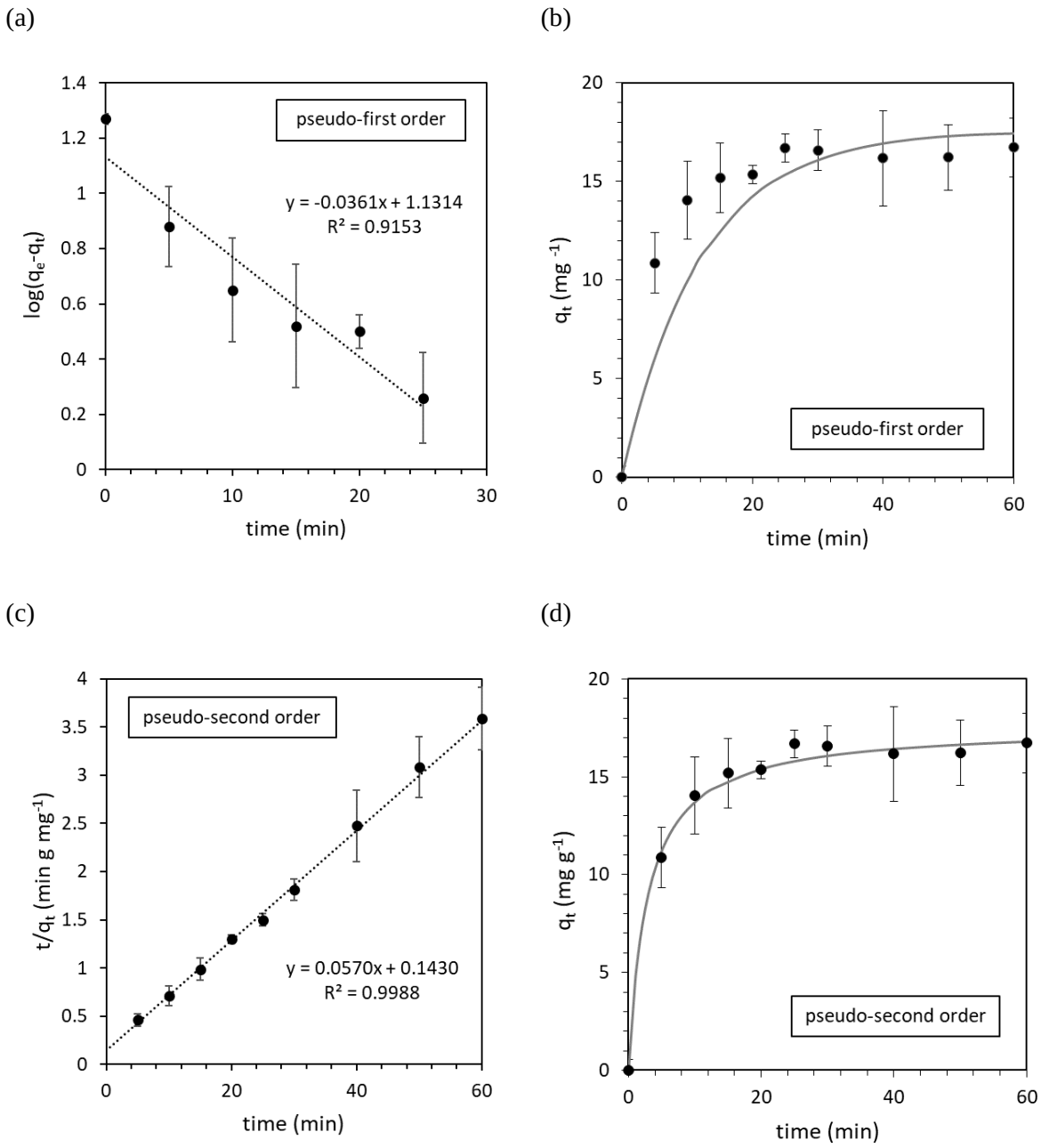

Figure 2: Kinetics of As(III) adsorption onto TiO_2-Fe_2O_3. Experimental conditions were pH 7 (0.01 M HEPES), with 39 mg L^{-1} initial As(III), and 1 g L^{-1} sorbent. Presented are both (a and b) pseudo-first order, and (c and d) pseudo-second order kinetic models, fitted to the experimental data. Error bars indicate the standard deviation between three repeat experiments.

The experimentally determined kinetic parameters are presented in Table 2. The PFO kinetic model gave a poor fit (R^2=0.7770), significantly underestimating the rate of adsorption in the first 20 minutes (Figure 2a and b).The PSO model, in contrast, provided a very accurate fit to experimental data (R^2 = 0.9928, Figure 2c and d). The PSO rate constant, k_2, was 0.020±0.002 g mg^{-1} min^1. This lies within the range of literature values for As(III) adsorption to similar multifunctional composite sorbents: 0.12 g mg^{-1} min^{-1} for γ-Fe_2O_3-TiO_2 [8] and 0.001 g mg^{-1} min^{-1} for γ-Fe_2O_3@ZrO_2 [47].

Table 2: Experimentally determined kinetic parameters for the adsorption of As(III) to TiO_2-Fe_2O_3. When kinetic data was linearised, R^2 values were 0.9153 for pseudo-first order kinetics and 0.9988 for pseudo-second order kinetics. Experimental conditions were 39 mg L^{-1} initial As(III), 1 g L^{-1} sorbent, pH 7 (0.01 M HEPES).

	Pseudo-first order	Pseudo-second order
Rate constant	k_1 = 0.083 ±0.019 min^{-1}	k_2 = 0.020 ±0.002 g mg^{-1} min^1
q_e (mg g^{-1})	17.6 ±0.6	17.6 ±0.3
R^2	0.7770	0.9928

3.3. Using a modified pseudo-second order (PSO) model for predictive modelling

We recently demonstrated that the pseudo-second order adsorption model can be modified to provide better sensitivity towards changes in C_0 and C_s [35]. The modified rate equation (Equation 1) uses a rate constant, k', that is readily calculated from experimental PSO parameters via Equation 2 [35]. Whilst the original PSO model provides no sensitivity towards C_0 and C_s, our modified model gives the first order dependence towards sorbate concentration, C_t, that is typically seen experimentally [35]. This model also incorporates sensitivity to C_s through the use of adsorption isotherms to determine q_e [35]. In this work, the Freundlich adsorption isotherm was used to calculate q_e, due to the possibility of multilayer As(III) sorption [46]. The modified kinetic model was validated through successful reconstruction of the original PSO model's fit to the experimental data (Figure 3Figure 3).

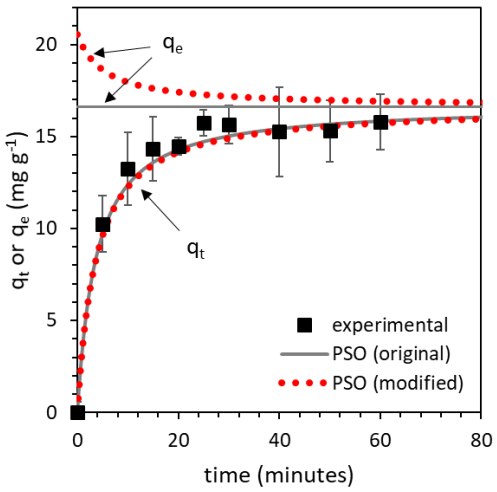

Figure 3: Comparison of the original PSO model with the modified kinetic adsorption model. The labels 'q_t' and 'q_e' indicate the quantity of adsorbed As(III) and the fixed or calculated value of q_e at each time point respectively. Note that the

magnitude of the Freundlich constant, K_F, has been increased (from 4.06 to 5.10) to account for the difference in q_e observed between the adsorption isotherm and kinetic experiments when C_e = 22.4 mg L^{-1} (in the Freundlich adsorption isotherm when C_e = 22.4 mg L^{-1}, q_e = 13.3 mg g^{-1}, in the kinetic experiments when C_e = 22.4 mg L^{-1}, q_e = 16.7 mg g^{-1}).

The models presented are labelled as follows: PSO (original): $\frac{dq_t}{d_t} = k_2(q_e - q_t)^2$ *, PSO (modified):* $\frac{dq}{d_t} = k'C_t\left(1 - \frac{q_t}{q_e}\right)^2$

where $k' = \frac{k_2 {q_e}^{\dagger 2}}{{C_0}^{\dagger}}$ *and q_e is calculated at each point in time using the Freundlich adsorption isotherm.*

3.4. Modelling the performance of an arsenic treatment plant: batch vs continuous-flow design

Input parameters for the kinetic adsorption model were determined experimentally at pH 7 using adsorption isotherms with C_e = 10-80 mg L^{-1} and C_s = 1 g L^{-1}, and adsorption kinetics with C_0 = 39 mg L^{-1} and C_s = 1 g L^{-1}. The modelling parameters are presented in Table 3. The neutral pH used is representative of typical groundwaters in South Asia and matches the point of zero charge for TiO_2-Fe_2O_3 (pH 7.0±0.2, Supplementary Information), and is thus appropriate for modelling small scale treatment systems where pH is not optimised. A relatively high value of C_0 used in the experimental work was chosen to increase accuracy and precision in the reported data, however it is over an order of magnitude greater than the C_0 values being modelled. The experimental sorbent loading, C_s (1 g L^{-1}), is at the upper end of typical photocatalyst concentrations and the bottom end of sorbent concentrations normally used for remediation via adsorption. This work therefore extrapolates outside the conditions used to experimentally determine the model parameters, and the results should be considered as giving a semi-quantitative or qualitative comparison of batch and continuous-flow systems, based on identifying appropriate orders of magnitude in sorbent concentrations and flow-rates for treatment plant design.

Table 3: Parameters used for kinetic adsorption modelling. The rate constant k' was determined from adsorption kinetics. Freundlich isotherm parameters were determined from adsorption isotherms, with K_F rescaled to account for the difference in q_e obtained between adsorption isotherms and adsorption kinetics. Errors indicate the 68% confidence interval.

Parameter	Label and units	Value
Rate constant	k' (L g^{-1} min^{-1})	0.111 ±0.015
Initial sorbate concentration	C_0 (μg L^{-1})	10-2000 (batch), 0 (continuous flow)
Initial sorbent concentration	C_s (g L^{-1})	0.01-10 000
Influent concentration	$C_{influent}$ (μg L^{-1})	0 (batch), 500, 1000 and 2000 (continuous flow)
Turnover rate	j (min^{-1})	0 (batch), 0.001–1 (continuous flow)
Adsorption capacity q_e (mg g^{-1})	K_F (mg g^{-1} (mg L^{-1}) $^{-1/n}$)	5.10 ±1.60
	n (unitless)	2.63 ±0.14

3.4.1. Batch reactor design

Batch reactors treat a single volume of water until contaminant concentrations are within safety limits. The user waits for the water to be treated before collection, with longer treatments allowing for more complete removal of contaminants. Results from the batch treatment model are presented in Figure 4, with kinetic profiles in Figure 4a, and the time required to provide safe drinking water (<10 μg L^{-1}) in Figure 4b. The model predicted that 0.1 g L^{-1} TiO_2-Fe_2O_3 could only successfully treat water contaminated with <100 μg L^{-1} As(III), and only with long treatment times on the hour timescale. At least 1 g L^{-1} TiO_2-Fe_2O_3 was needed to treat As(III) contaminated water within 1 hour, and even then, several hours of treatment was needed when C_0 was greater than 400 μg L^{-1}. With ≥10 g L^{-1} sorbent, water contaminated with up to 2000 μg L^{-1} As(III) was rapidly remediated within a matter of minutes.

This model suggests that for batch treatments using multi-functional photocatalyst-sorbent materials, more than the typical 0.01-0.1 g L^{-1} photocatalyst loading is required for the sorbent to perform sufficiently. Furthermore, below 1 g L^{-1} kinetic limitations are important, adding constraints on treatment time.

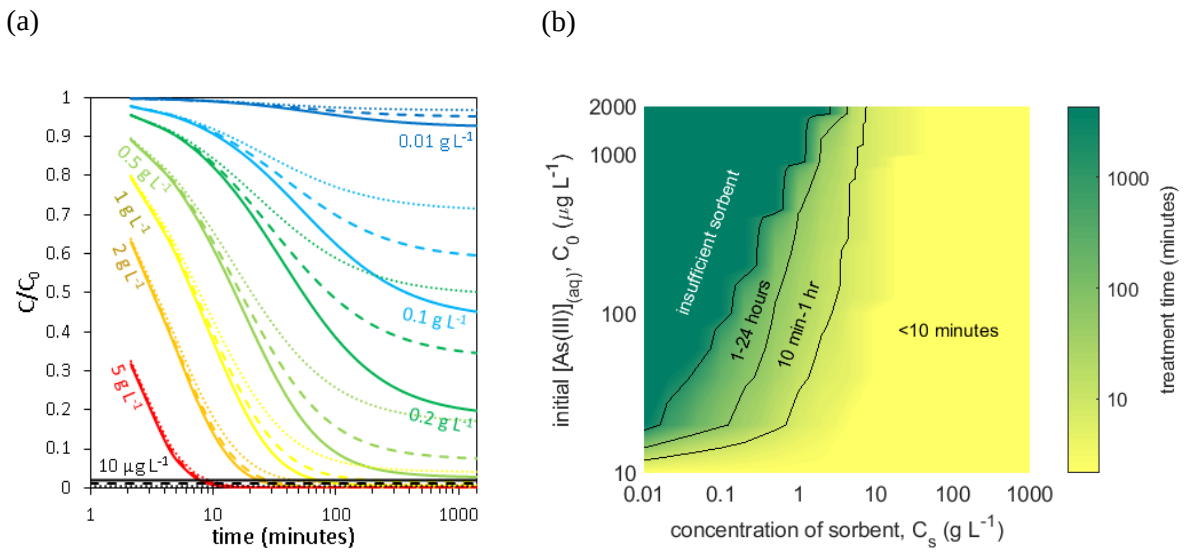

Figure 4: Modelling batch treatments. (a) Batch kinetics predicted for As(III) adsorption using different sorbent loadings of TiO_2-Fe_2O_3. The simulated kinetics are shown for initial As(III) concentrations of 500 µg L^{-1} (solid lines), 1000 µg L^{-1} (dashed lines) and 2000 µg L^{-1} (dotted lines). The black lines close to the x-axis indicate the 10 µg L^{-1} WHO arsenic guideline limit. (b) The time taken to remove arsenic below the 10 µg L^{-1} WHO limit, as a function of both initial As(III) concentration and sorbent loading. C_s refers to sorbent concentration and $[As(III)]_0$ is the initial concentration of aqueous As(III), C_0.

3.4.2. Continuous-flow reactor design

In a continuous-flow system, contaminated influent is continuously pumped into the reactor whilst treated effluent is extracted. Breakthrough curves for the continuous-flow model are given in Figure 5(a) and (b). At high sorbent concentrations (≥100 g L^{-1}), varying the turnover rate between 0.001 and 0.1 min^{-1} had little effect on the shape of the simulated breakthrough curve: the sorbent removed As(III) sufficiently fast that no build-up of aqueous As(III) in the reactor occurred prior to sorbent saturation. For more dilute TiO_2-Fe_2O_3 suspensions (≤10 g L^{-1}), however, the shape of the breakthrough curve in our model was strongly influenced by the turnover rate.

For instance, when modelling suspensions of 10 g L^{-1} sorbent, under a slow turnover rate of 0.001 min^{-1}, breakthrough only occurred once the sorbent was saturated. With an influent of 500 μg L^{-1} As(III) this corresponds to breakthrough (above the WHO limit of 10 μg L^{-1}) after 14 bed volumes (Figure 5c). When turn over frequency was increased to 0.01 min^{-1}, fewer bed volumes were treated before breakthrough due to kinetic limitations: breakthrough was reached after just 6 bed volumes. Formation of a steady state before breakthrough was also observed, with 4.5 μg L^{-1} As(III) in the reactor. When turnover frequency was increased to 0.1 min^{-1}, breakthrough was reached after just 2.6 bed volumes. Here, the model predicted a steady state scenario with approximately 43 μg L^{-1} As(III), already exceeding the WHO limit. Since breakthrough occurred with an unsaturated sorbent, due to the As(III) steady-state, this scenario represents an inefficient and uneconomical use of sorbent. Similar results were observed with 2,000 μg L^{-1} (Figure 5d), however the higher influent concentration leads to As(III) steady-states surpassing the guideline limits at lower turnover rates.

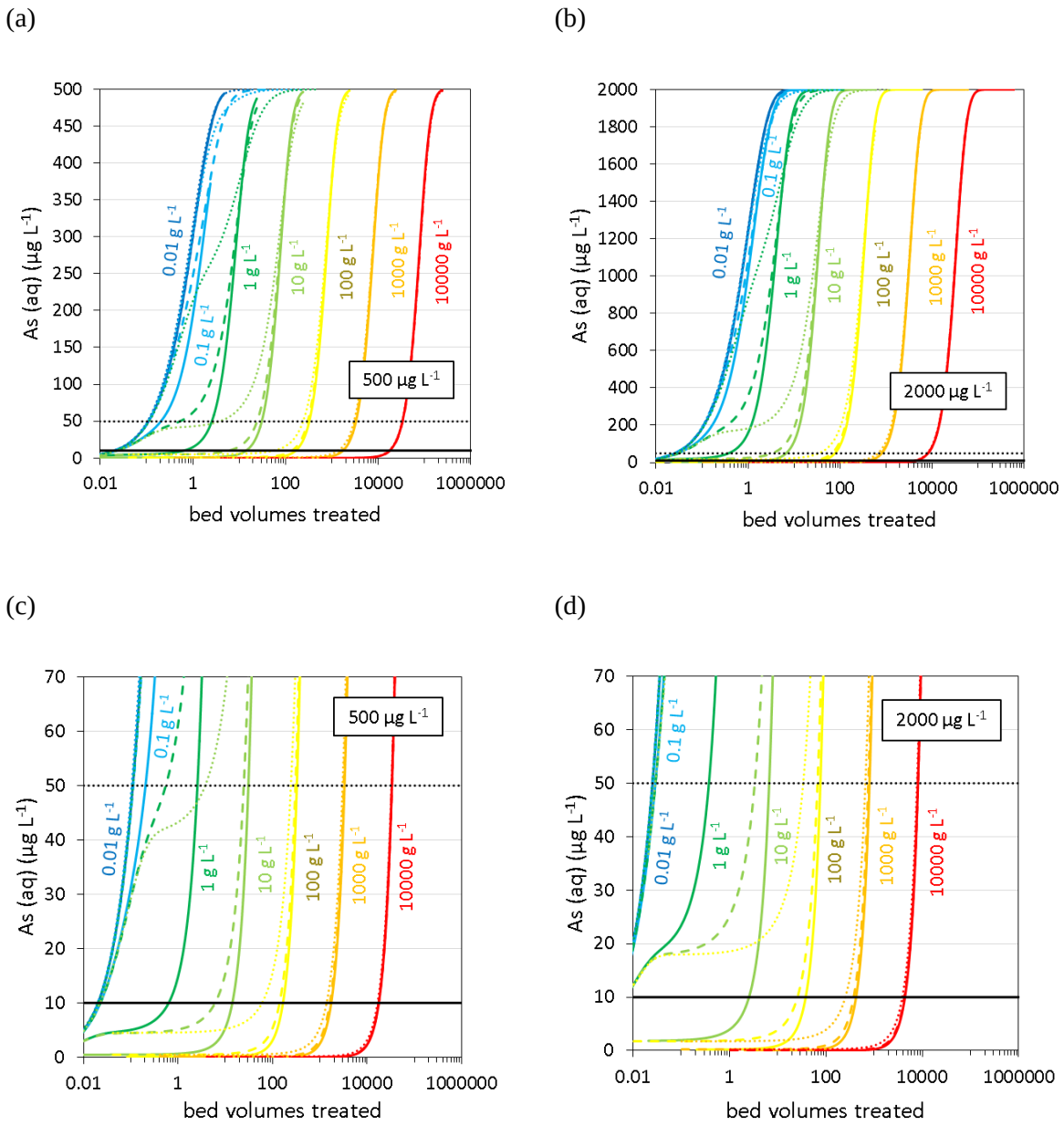

Figure 5: Modelling continuous-flow treatments. Simulated As(III) breakthrough curves as a function of sorbent loading are presented with influent concentrations of (a) 500 µg L^{-1} and (b) 2000 µg L^{-1} As(III). (c) and (d) provide close ups of arsenic breakthrough and the formation of steady-states. Breakthrough curves were simulated at turnover rates of 0.001 (solid lines), 0.01 (dashed lines) and 0.1 (dotted lines) min^{-1}. Both the WHO 10 µg L^{-1} guideline limit (solid black lines) and the higher 50 µg L^{-1} limit (dashed black lines) are indicated.

The results predicted by our model match experimental observations in similar systems: breakthrough at under-saturated conditions due to high flow-rates in the adsorption of As(V) to laterite [52], and steady-state breakthrough during As(V) adsorption to both two-line ferrihydrite (an iron oxide) [53], and anion exchange beads [54]. Ideally, the sorbent is saturated at breakthrough: this is a more

economical use of material, with the sorbent requiring replacement less often. The simulated results suggested that aiming to achieve a sorbent efficiency of at least 50%, with <10 μg L^{-1} As(III) in the effluent, and a turnover rate of 0.01-0.1 min^{-1} (i.e. between 10 and 100 minutes treatment time), sorbent concentrations in the order of 100 g L^{-1} are needed to treat 500 μg L^{-1} influent As(III), and 1000 g L^{-1} sorbent is needed to treat 2000 μg L^{-1} influent As(III).

3.4.3. Comparison of reactor designs

A comparison between simulated results using the batch and continuous-flow treatment models is given in Figure 6, showing both turnover rate (the reciprocal of treatment time, on the left-hand y-axis) and sorbent efficiency (as the quantity of sorbate adsorbed after successful treatment, or at breakthrough, on the right-hand y-axis) as a function of sorbent loading. For the continuous-flow system, the reported data was selected to give the best combination of turnover rate and sorbent efficiency (calculated as the product between the two).

For the batch treatment, the model gave a linear relationship between increasing C_s and turnover rate, since the rate of As(III) removal in the model is first order with respect to C_s. The sorbent efficiency linearly decreased with increasing C_s, as the same quantity of arsenic in the reactor becomes distributed across an increasingly large sorbent mass.

The continuous-flow system also showed a linear increase between C_s and turnover rate, again due to the first order dependence of adsorption rate upon C_t within the model. However, unlike the batch system, the sorbent efficiency of continuous-flow treatment increased with increasing C_s. This was because at low values of C_s, breakthrough occurred with undersaturated sorbent, due to slow adsorption kinetics. At high values of C_s, kinetic limitations become less significant and the sorbent reached a higher degree of saturation before breakthrough.

As indicated by the stars in Figure 6, the continuous-flow system was predicted to require between one and two orders of magnitude more sorbent (g L^{-1}) than the batch system to achieve the same sorbent efficiency (mg g^{-1}) at similar turnover rates (min^{-1}). For example, in the batch treatment, 10 g L^{-1} sorbent

was sufficient to treat water contaminated with up to 2,000 μg L^{-1} As(III) in less than ten minutes (i.e. a turnover rate of 0.1 $minute^{-1}$), whereas in the continuous flow model 1,000 g L^{-1} was needed. This is logical, since in the batch treatment the entire quantity of sorbate is introduced to the sorbent at once, leading to much faster early adsorption kinetics (due to the first order dependency on C_t). The continuous-flow scenario is different, as the concentration of aqueous As(III) at each point in time (C_t) can never exceed 10 μg L^{-1} As(III) without breakthrough having been reached. The difference between batch and continuous-flow systems becomes more pronounced at higher sorbate concentrations, as the difference in C_t at t=0 between batch and continuous-flow systems becomes more significant. The implication is that batch treatment may be more appropriate for scenarios requiring low sorbent concentrations (such as when using photocatalysis) and requiring a very large reduction in the relative concentration of contaminants (e.g. reducing 2,000 μg L^{-1} As(III) to just 10 μg L^{-1}). These results suggest that for a one-off remediation, batch treatment is more appropriate than continuous-flow, with faster treatment times and the same sorbent efficiencies, but only if the appropriate mass of sorbent can be identified to minimise surplus sorbent and thus achieve good sorbent economies.

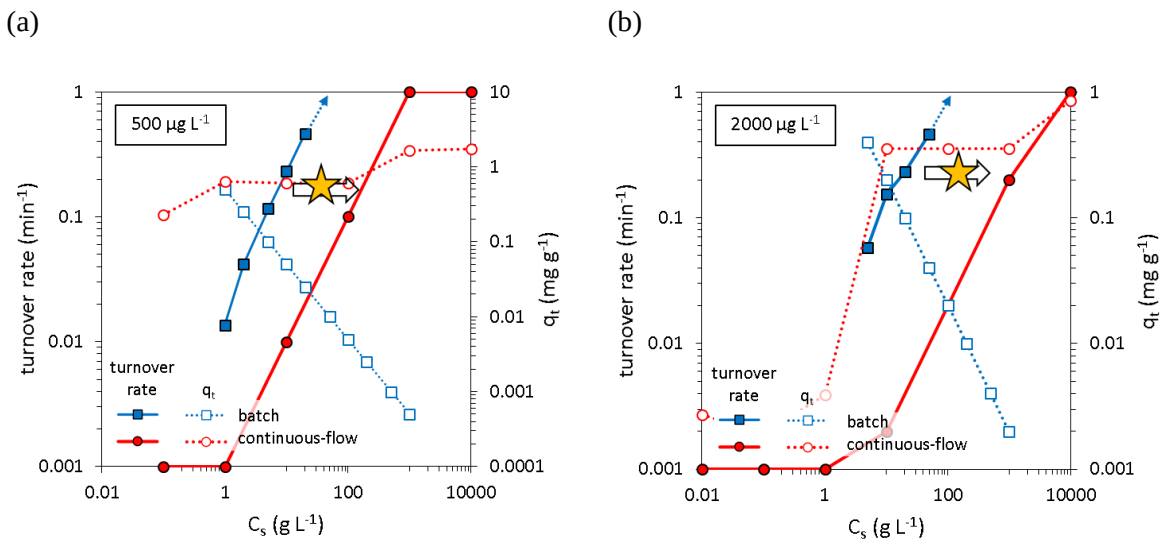

Figure 6: Comparison of simulated results for batch (blue squares) and continuous-flow (red circles) treatments. Turnover rate (filled shapes and solid lines) and sorbent efficiency (open shapes, dotted lines) are given as a function of sorbent loading. For the continuous-flow system, a two-dimensional matrix of experiments, varying in C_s and turnover rate, was simulated. To reduce the two independent variables to just one (C_s), the data shown corresponds to the 'optimum' turnover rate identified at each value of C_s, determined as the value of turnover rate giving the highest product of j and q_t, i.e. an equal priority

weighting for turnover rate and sorbent efficiency. The arrow labelled with a star denotes the shift in sorbent concentration required to achieve similar performance (turnover and sorbent efficiencies) between continuous-flow and batch treatment systems.

3.5. Modelling a 365-day deployment

3.5.1. Daily household water requirements and boundary conditions

As discussed, historic failings of South Asia mitigation schemes designed around sorbent filters include the difficulty users find when cleaning saturated media [16], carrying out maintenance, and the limited market availability of fresh sorbent media to replace saturated media [24] [17]. Here, we therefore wanted to explore how batch and continuous-flow treatments would compare if the sorbent were used for an entire year before replenishment. The best solution would provide safe, potable water (<10 $\mu g\ L^{-1}$ arsenic) for 365 days, using the least sorbent, due to the need for cost efficiency [16].

As boundary conditions for the volume of potable water required, we considered the needs of a rural family in West Bengal, India, with an average of 5.7 people per household [55]. The WHO South-East Asia Technical Office reports that 7 litres of water is required per person per day (4 L per capita per day (Lpcd) for drinking and 3 Lpcd for food preparation) [56]. These two figures give a requirement of 40 L day^{-1} potable water per household. This is equivalent to 14,600 L per year per household, and where C_0=500 $\mu g\ L^{-1}$ As(III), equates to the removal of 7.3 grams of arsenic per year. Flow rate was not considered an essential parameter, as whilst the WHO specifies that the flow rate at each collection point should be at least 0.125 litres per second [56], in cases where treatment is slow, effluent can be collected in a storage tank prior to distribution, as is in current treatment plants [20].

3.5.2. Modelling sequential batch treatments

To model a 365-day deployment, the continuous-flow MATLAB code was used without modification. For the batch treatment system, codes were modified to represent gradual saturation of the media during 365 sequential treatments. A selection of simulated results presented are Figure 7, highlighting the inverse relationship between initial sorbate concentration, C_0, and the number of days successfully treated.

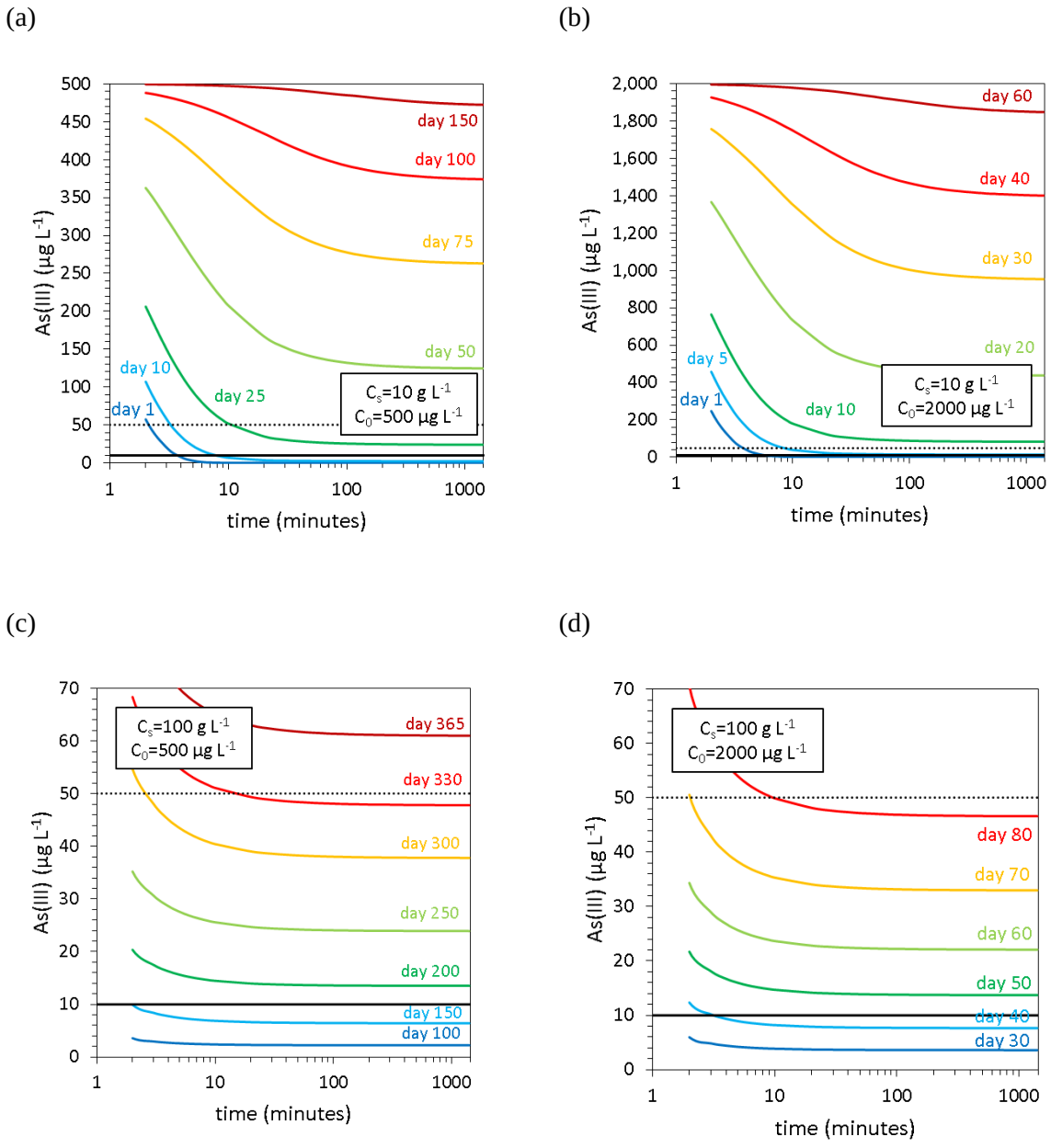

Figure 7: Kinetic adsorption modelling: batch treatment using the same sorbent for 365 days. Shown are kinetic profiles for simulations using 10 g L^{-1} sorbent and initial As(III) concentrations of 500 (a), and 2000 (b) µg L^{-1}, and 100 g L^{-1} sorbent with

initial As(III) concentrations of (c) 500, and (d) 2000 μg L^{-1}. For each simulation after day 1, the initial amount of adsorbed As(III) (q_t) was set as the final value of q_t for the simulation representing the previous day, reflecting the sorbent becoming saturated through repeat use. The WHO 10 μg L^{-1} guideline limit (solid black lines) 50 μg L^{-1} limit (dashed black lines) are indicated.

3.5.3. Comparison of batch and continuous-flow treatments

The 365-day models predicted that the batch treatment would provide safe water for at least as many days as the continuous-flow design under all combinations of C_s and treatment time (Table 4). For the batch reactor, the number of days per year with successful As(III) removal depended primarily on sorbent loading and was not significantly affected by the treatment time: batch treatment was rapid due to the fast kinetics during initial mixing, resulting from the high initial concentration of As(III) and first order dependence on C_t. However, for the continuous-flow reactor, sorbent loading and flow rate (turnover rate) were equally important; for instance, reducing the flow rate by a factor of 10 had the same effect on the number of days with successful treatment as multiplying the sorbent concentration by a factor of 10. This was due to high turnover rates (short residence times) leading to As(III) breakthrough before the sorbent was saturated: the concentration of As(III) in the continuous-flow reactor was always <10 μg L^{-1} before breakthrough, and adsorption kinetics were therefore limited by the first order dependence on C_t.

The model suggested that the batch reactor would prove more successful when treatment times are shortened. For instance, in the batch model, 100 g L^{-1} sorbent successfully removed 500 μg L^{-1} As(III) for 175 days with a treatment time of just 20 minutes per day (Table 4). In contrast, 100 g L^{-1} sorbent in the continuous-flow system failed to treat water contaminated with 500 μg L^{-1} As(III) with 20 minutes average residence time after just one day (Table 4). The implication is that batch reactor designs may be more economical: shorter treatment times in a batch reactor mean that energy intensive processes such as pumping, mixing and ultraviolet irradiation might be performed for shorter durations.

Table 4: Comparison of results from modelling 365-day sorbent deployments in batch and continuous-flow configurations. Presented are the number of days during which water was successfully treated for (a) batch and (b) continuous-flow systems as a function of sorbent loading and the average residence time, with 500 μg L^{-1} initial As(III). The colour transition between red, yellow and green reflects increasing life-times of the reactor before breakthrough (with a maximum of 365).

Batch treatment								Continuous-flow treatment							
Treatment time (minutes)	Sorbent concentration (g L^{-1})							Residence time (minutes)	Sorbent concentration (g L^{-1})						
	0.01	0.1	1	10	100	1000	10000		0.01	0.1	1	10	100	1000	10000
1	0	0	0	0	100	365	365	1	0	0	0	0	0	1	12
2	0	0	0	0	150	365	365	2	0	0	0	0	0	1	21
5	0	0	0	5	150	365	365	5	0	0	0	0	0	4	56
10	0	0	0	10	150	365	365	10	0	0	0	0	0	10	115
20	0	0	0	15	175	365	365	20	0	0	0	0	1	21	236
50	0	0	0	15	175	365	365	50	0	0	0	0	4	56	365
100	0	0	1	17	175	365	365	100	0	0	0	0	10	115	365
200	0	0	1	17	175	365	365	200	0	0	0	1	21	236	365
500	0	0	1	17	175	365	365	500	0	0	0	4	56	365	365
1000	0	0	1	17	178	365	365	1000	0	0	0	10	115	365	365

3.5.4. Economising sorbent use

A minimum sorbent concentration of 1 kg L^{-1} was required to safely remove As(III) for an entire year in both reactor designs. This is much higher than typical photocatalyst concentrations. Whilst treatments in the hours timescale were needed for continuous-flow, batch treatment was successful in just minutes. However, the best sorbent economies were achieved under conditions wherein the sorbent needed replacing during the 365-day deployment (Figure 8). At the slowest treatment times (1,000 minutes, approximating a reactor operated continuously all day), batch treatments gave the best sorbent economy

when sorbent concentration was less than 100 g L^{-1}, whilst continuous-flow treatments gave a better sorbent economy with C_s >100 g L^{-1} (Figure 8). Further results on sorbent economy are given in the Supplementary Information.

The minimum mass of sorbent required was similar between batch and continuous-flow models, with 8.2 and 8.4 kg sorbent household^{-1} year^{-1} respectively (when initial As(III) was 500 μg L^{-1}). However, the conditions under which optimal sorbent economies were obtained varied between the two systems. Sorbent economy was best in the batch model when using 100 g L^{-1} sorbent and treatment times of 1000 minutes (8.2 kg sorbent household^{-1} year^{-1}), however similar results were achieved with less sorbent and faster treatment times: 10 g L^{-1} sorbent and 100 minutes treatment times gave a sorbent requirement of 8.6 kg household year^{-1}. When C_s = 10 g L^{-1} and 100 g L^{-1}, the sorbent required replacing every 17 and 175 days respectively. In the continuous-flow model, the best sorbent economy was achieved with much higher sorbent concentrations: C_s = 1 and 10 kg L^{-1}, and treatment times of 200 and 20 minutes respectively. Under these conditions 8.6 kg sorbent household^{-1} year^{-1} was required and the sorbent would require replacing every 236 days. The batch model therefore provided better sorbent economies at low sorbent concentrations, again suggesting that this is the more appropriate reactor design for photocatalyst-sorbent systems.

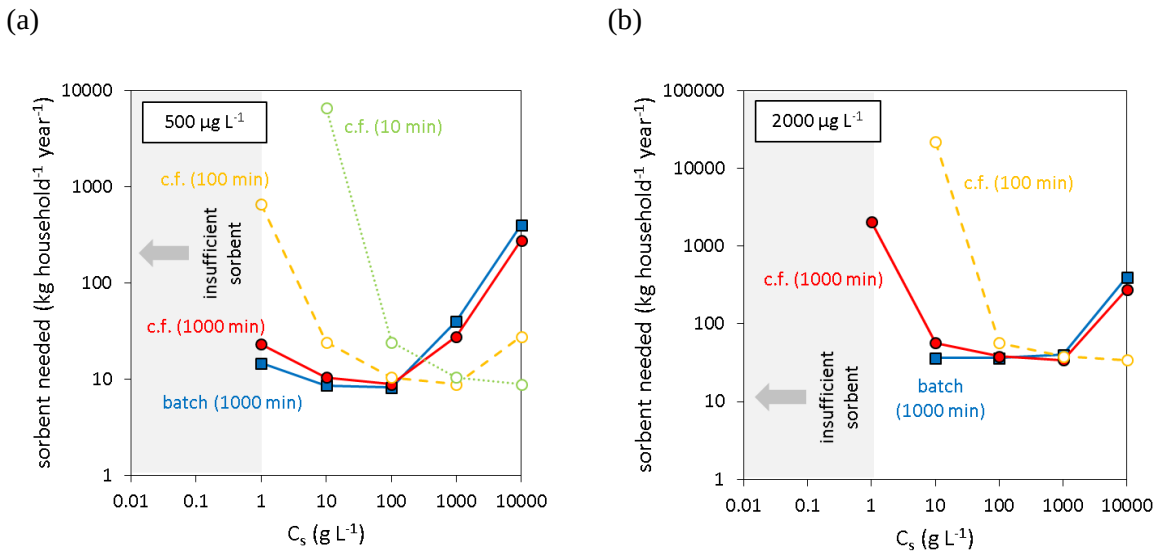

Figure 8: Comparison of results from modelling 365-day sorbent deployments in batch and continuous-flow configurations. Sorbent efficiency (kg sorbent required per household per year) is presented as a function of sorbent concentration, and with different treatment times, where initial As(III) concentrations are (a) 500 µg L^{-1} and (b) 2000 µg L^{-1}. Note that some data points correspond with scenarios wherein the sorbent has failed to provide 365 days of safe water. Continuous-flow is abbreviated as 'c.f.', the batch model is given as blue squares, and continuous-flow as (i) red circles-solid lines (1000 minutes average residence time), (ii) open circles-yellow dashed lines (100 minutes) and (iii) open circles-green dotted lines (10 minutes).

The ~8 kg of sorbent per household per year is only an estimation, as a number of factors will affect the true amount of sorbent needed. For instance, As(III) has been considered in the absence of competitor ions which supress adsorption. Secondly, multilayer surface precipitation effects are important for both As(III) and As(V), increasing arsenic removal [46] [57]. Surface precipitation is a much slower process than adsorption and is thus unlikely to have been captured in our experimental determination of As(III) adsorption kinetics.

3.6. Implications for engineering photocatalyst-sorbent systems

The simulated models suggested that batch treatments are more efficient than continuous-flow when the sorbent concentration is limited (i.e. <10 g L^{-1}), for both single use and long-term deployment. Since most applications of photocatalysts for water remediation use low catalyst concentrations, the batch

reactor design appears most promising for the application of multifunctional composite-sorbents such as TiO_2-Fe_2O_3. The model also suggested that more than 100 g L^{-1} is required for a year's treatment without changing media, much higher than typical photocatalyst concentrations. To operate at 1 g L^{-1} and under, the TiO_2-Fe_2O_3 media would thus need to be replenished several times per year.

The batch reactor design is 'safer' in the sense that there is less dependency on treatment time (due to fast removal in the initial minutes of treatment thanks to high C_t), with sorbent loading being the principal parameter. By using excess concentrations of sorbent, water can be treated rapidly without breakthrough. Our results contrast with Lekić et al. who observed experimentally that As(III) and As(V) removal per gram of sorbent was superior in a column (continuous-flow) configuration compared with batch treatment, which they posited as being due to non-adsorption processes such as coagulation, flocculation and filtration, that were not included in our present model [23]. Our recommendation is thus that photooxidation kinetics in the photocatalyst-sorbent system be studied at high material concentrations $\geq$10 g L^{-1}, and with different reactor dimensions, to verify that suspensions can be sufficiently irradiated to provide effective photooxidation at the high sorbent concentrations needed to achieve sufficient device lifetimes.

4. Conclusions

This work aimed to address the question of how much sorbent is needed in a reactor for As(III) remediation based on TiO_2-Fe_2O_3 composite photocatalyst-sorbent technology. We considered the conservative scenario that the material is acting as a sorbent only. Our findings are that:

a) Material loading significantly greater than the 0.01-0.1 g L^{-1} concentrations of photocatalysts normally used in the literature are needed for TiO_2-Fe_2O_3 to effectively remove As(III) from contaminated waters through adsorption;
b) Kinetic modelling predicts that batch treatment processes are preferred over continuous flow for the adsorption of As(III) at sorbent concentrations <100 g L^{-1}. Batch processes should be considered in preference to continuous-flow, given that sorbent concentrations should be minimised to provide sufficient penetration of light through suspension;
c) With 10 g L^{-1} TiO_2-Fe_2O_3 or less, the media would need to be replenished multiple times throughout the year to maintain effective treatment;
d) Continuous flow only offers more economical use of sorbent at high sorbent loading (>100 g L^{-1}).

On the basis of this study, we recommend subsequent experimental work on multifunctional photocatalyst-sorbent materials to consider the influence of material concentration on photooxidation kinetics, given that concentrations of ≥10 g L^{-1} may be required for effective adsorption of contaminants such as arsenic. An experimental comparison of batch and continuous-flow reactors using photocatalyst-sorbent technology is required. This kinetic adsorption model may be further advanced through introduction of experimental photooxidation rates to provide further insight as to how photocatalyst-sorbent materials might be applied in engineered applications towards the remediation of As(III) contaminated waters.

5. Acknowledgements

The authors acknowledge support from the Engineering Physical Sciences Research Council (EPSRC) [grant number EP/N509486/1], the William J Kenan Charitable Trust, the Royal Thai Government and from the University of Phayao. The authors also thank Dr Jens Narkoja from the Natural History Museum, UK, for providing XRD analysis.

6. References

[1] A. Kumar, M. Biswas, P.K. Roy, J.M. Wallace, Assessment of Arsenic Removal Units in Arsenic-Prone Rural Area in Uttar Pradesh , India, J. Inst. Eng. Ser. A. (2019). https://doi.org/10.1007/s40030-018-0349-9.

[2] J.G. Hering, I.A. Katsoyiannis, G.A. Theoduloz, M. Berg, S.J. Hug, Arsenic removal from drinking water: Experiences with technologies and constraints in practice, J. Environ. Eng. (United States). 143 (2017) 1–9. https://doi.org/10.1061/(ASCE)EE.1943-7870.0001225.

[3] S. Sorlini, F. Gialdini, Conventional oxidation treatments for the removal of arsenic with chlorine dioxide, hypochlorite, potassium permanganate and monochloramine, Water Res. 44 (2010) 5653–5659. https://doi.org/10.1016/j.watres.2010.06.032.

[4] V.K. Sharma, M. Sohn, Aquatic arsenic: Toxicity, speciation, transformations, and remediation, Environ. Int. 35 (2009) 743–759. https://doi.org/10.1016/j.envint.2009.01.005.

[5] E.E. Lavonen, M. Gonsior, L.J. Tranvik, P. Schmitt-Kopplin, S.J. Köhler, Selective chlorination of natural organic matter: Identification of previously unknown disinfection byproducts, Environ. Sci. Technol. 47 (2013) 2264–2271. https://doi.org/10.1021/es304669p.

[6] Z. Zhang, J. Gamage, Applications of photocatalytic disinfection, Int. J. Photoenergy. 2010 (2010). https://doi.org/10.1155/2010/764870.

[7] W. Zhou, H. Fu, K. Pan, C. Tian, Y. Qu, P. Lu, C. Sun, Mesoporous TiO2/α-Fe2O3: Multifunctional Composites for Effective Elimination of Arsenite Contamination through Simultaneous Photocatalytic Oxidation and Adsorption, J Phys Chem. 112 (2008) 19584–19589. https://doi.org/10.1021/jp806594m.

[8] L. Yu, X. Peng, F. Ni, J. Li, D. Wang, Z. Luan, Arsenite removal from aqueous solutions by γ-Fe2O3-TiO2 magnetic nanoparticles through simultaneous photocatalytic oxidation and adsorption, J. Hazard. Mater. 246–247 (2013) 10–17.

https://doi.org/10.1016/j.jhazmat.2012.12.007.

[9] H. Su, X. Lv, Z. Zhang, J. Yu, T. Wang, Arsenic removal from water by photocatalytic functional Fe2O3–TiO2 porous ceramic, J. Porous Mater. 24 (2017) 1227–1235. https://doi.org/10.1007/s10934-017-0362-9.

[10] R.I. Bickley, M.J. Slater, W.J. Wang, Engineering development of a photocatalytic reactor for waste water treatment, Process Saf. Environ. Prot. 83 (2005) 205–216. https://doi.org/10.1205/psep.04028.

[11] A. Yerkinova, G. Balbayeva, V.J. Inglezakis, S.G. Poulopoulos, Photocatalytic Treatment of a Synthetic Wastewater, IOP Conf. Ser. Mater. Sci. Eng. 301 (2018). https://doi.org/10.1088/1757-899X/301/1/012143.

[12] C. Ferreiro, N. Villota, J.I. Lombraña, M.J. Rivero, V. Zúñiga, J.M. Rituerto, Analysis of a hybrid suspended-supported photocatalytic reactor for the treatment of wastewater containing benzothiazole and aniline, Water (Switzerland). 11 (2019). https://doi.org/10.3390/w11020337.

[13] P.K. Dutta, S.O. Pehkonen, V.K. Sharma, A.K. Ray, Photocatalytic oxidation of arsenic(III): Evidence of hydroxyl radicals, Environ. Sci. Technol. 39 (2005) 1827–1834. https://doi.org/10.1021/es0489238.

[14] V. Vaiano, G. Iervolino, D. Sannino, L. Rizzo, G. Sarno, A. Farina, Enhanced photocatalytic oxidation of arsenite to arsenate in water solutions by a new catalyst based on MoOx supported on TiO2, Appl. Catal. B Environ. 160–161 (2014) 247–253. https://doi.org/10.1016/j.apcatb.2014.05.034.

[15] E. Colombo, M. Ashokkumar, Comparison of the photocatalytic efficiencies of continuous stirred tank reactor (CSTR) and batch systems using a dispersed micron sized photocatalyst, RSC Adv. 7 (2017) 48222–48229. https://doi.org/10.1039/c7ra09753k.

[16] R.B. Johnston, S. Hanchett, M.H. Khan, The socio-economics of arsenic removal, Nat. Geosci. 3 (2010) 2–3. https://doi.org/10.1038/ngeo735.

[17] M. Shafiquzzaman, M.S. Azam, I. Moshima, J. Nakajima, Technical and Social evaluation of arsenic mitigation in rural bangladesh, J. Heal. Popul. Nutr. 27 (2009) 674–683. https://doi.org/10.3329/jhpn.v27i5.3779.

[18] M.S. German, T.A. Watkins, M. Chowdhury, P. Chatterjee, M. Rahman, Evidence of Economically Sustainable Village-Scale Microenterprises for Arsenic Remediation in Developing Countries, Env. Sci.Technol. (2019). https://doi.org/10.1021/acs.est.8b02523.

[19] A.B. Dichiara, S.J. Weinstein, R.E. Rogers, On the Choice of Batch or Fixed Bed Adsorption Processes for Wastewater Treatment, Ind. Eng. Chem. Res. 54 (2015) 8579–8586. https://doi.org/10.1021/acs.iecr.5b02350.

[20] A. Bhardwaj, R. Rajput, K. Misra, Status of Arsenic Remediation in India, Elsevier Inc., 2019. https://doi.org/10.1016/b978-0-12-814790-0.00009-0.

[21] C. McCullagh, N. Skillen, M. Adams, P.K.J.J. Robertson, Photocatalytic reactors for environmental remediation: A review, J. Chem. Technol. Biotechnol. 86 (2011) 1002–1017. https://doi.org/10.1002/jctb.2650.

[22] I. Ali, Z.A. Al-Othman, A. Alwarthan, M. Asim, T.A. Khan, Removal of arsenic species from water by batch and column operations on bagasse fly ash, Environ. Sci. Pollut. Res. 21 (2014) 3218–3229. https://doi.org/10.1007/s11356-013-2235-3.

[23] B.M. Lekić, D.D. Marković, V.N. Rajaković-Ognjanović, A.R. Dukić, L. V. Rajaković, Arsenic removal from water using industrial By-products, J. Chem. 2013 (2013). https://doi.org/10.1155/2013/121024.

[24] D.K. Kundu, A.P.J. Mola, A. Gupta, Failing arsenic mitigation technology in rural Bangladesh: Explaining stagnation in niche formation of the Sono filter, Water Policy. 18 (2016) 1490–1507. https://doi.org/10.2166/wp.2016.014.

[25] The Failing Response to Arsenic in the Drinking Water of Bangladesh's Rural Poor | HRW, (n.d.). https://www.hrw.org/report/2016/04/06/nepotism-and-neglect/failing-response-arsenic-

drinking-water-bangladeshs-rural (accessed June 15, 2017).

[26] S.R. Khandker, H.A. Samad, R. Ali, D.F. Barnes, Who benefits most from rural electrification? Evidence in India, Energy J. (2014). https://doi.org/10.5547/01956574.35.2.4.

[27] M. D'Arcy, D. Weiss, M. Bluck, R. Vilar, Adsorption kinetics, capacity and mechanism of arsenate and phosphate on a multifunctional TiO2-Fe2O3 bi-composite, J. Colloid Interface Sci. 364 (2011) 205–212. https://doi.org/10.1016/j.jcis.2011.08.023.

[28] K. Liu, H. Fu, K. Shi, F. Xiao, L. Jing, B. Xin, Preparation of large-pore mesoporous nanocrystalline TiO2 thin films with tailored pore diameters, J. Phys. Chem. B. 109 (2005) 18719–18722. https://doi.org/10.1021/jp054546p.

[29] N. Ayawei, A.N. Ebelegi, D. Wankasi, Modelling and Interpretation of Adsorption Isotherms, J. Chem. 2017 (2017). https://doi.org/10.1155/2017/3039817.

[30] Y.S. Ho, G. McKay, Pseudo-second order model for sorption processes, Process Biochem. 34 (1999) 451–465. https://doi.org/10.1016/S0032-9592(98)00112-5.

[31] K. Gibbon-Walsh, P. Salaün, M.K. Uroic, J. Feldmann, J.M. McArthur, C.M.G. Van Den Berg, Voltammetric determination of arsenic in high iron and manganese groundwaters, Talanta. 85 (2011) 1404–1411. https://doi.org/10.1016/j.talanta.2011.06.038.

[32] A. Cheng, R. Tyne, Y.T. Kwok, L. Rees, L. Craig, C. Lapinee, M. D'Arcy, D.J. Weiss, P. Salaün, Investigating Arsenic Contents in Surface and Drinking Water by Voltammetry and the Method of Standard Additions, J. Chem. Educ. (2016) acs.jchemed.6b00025. https://doi.org/10.1021/acs.jchemed.6b00025.

[33] J.C. Bullen, A. Torres-huerta, P. Salaün, J.S. Watson, S. Majumdar, R. Vilar, D.J. Weiss, Portable and rapid arsenic speciation in synthetic and natural waters by an As(V)-selective chemisorbent, validated against anodic stripping voltammetry, Water Res. 175 (2020) 115650. https://doi.org/10.1016/j.watres.2020.115650.

[34] W. Hu, J. Xie, H.W. Chau, B.C. Si, Evaluation of parameter uncertainties in nonlinear regression

using Microsoft Excel Spreadsheet, Environ. Syst. Res. 4 (2015). https://doi.org/10.1186/s40068-015-0031-4.

[35] J.C. Bullen, S. Saleesongsom, D.J. Weiss, A revised pseudo-second order kinetic model for adsorption, sensitive to changes in sorbate and sorbent concentrations, ChemRxiv Prepr. (2020). https://doi.org/10.26434/chemrxiv.12008799.

[36] A.W. Marczewski, Analysis of kinetic langmuir model. Part I: Integrated kinetic langmuir equation (IKL): A new complete analytical solution of the langmuir rate equation, Langmuir. 26 (2010) 15229–15238. https://doi.org/10.1021/la1010049.

[37] Y. Huang, M.U. Farooq, S. Lai, X. Feng, P. Sampranpiboon, X. Wang, W. Huang, Model fitting of sorption kinetics data: Misapplications overlooked and their rectifications, AIChE J. 64 (2018) 1793–1805. https://doi.org/10.1002/aic.16051.

[38] J.C. Bullen, MATLAB codes - A kinetic adsorption model for modelling Arsenic Treatment Plant (ATP) lifetimes, (2020). https://doi.org/10.5281/zenodo.3690170.

[39] D. Chakraborti, M.M. Rahman, A. Mukherjee, M. Alauddin, M. Hassan, R.N. Dutta, S. Pati, S.C. Mukherjee, S. Roy, Q. Quamruzzman, M. Rahman, S. Morshed, T. Islam, S. Sorif, M. Selim, M.R. Islam, M.M. Hossain, Groundwater arsenic contamination in Bangladesh-21 Years of research, J. Trace Elem. Med. Biol. 31 (2015) 237–248. https://doi.org/10.1016/j.jtemb.2015.01.003.

[40] K.K. Gupta, N.L. Singh, A. Pandey, S.K. Shukla, S.N. Upadayay, V. Mishra, P. Srivastava, N.P. Lalla, P.K. Mishra, Effect of Anatase/Rutile TiO2 Phase Composition on Arsenic Adsorption, J. Dispers. Sci. Technol. 34 (2013) 1043–1052. https://doi.org/10.1080/01932691.2012.735937.

[41] W. Tang, Q. Li, S. Gao, J.K. Shang, Arsenic (III,V) removal from aqueous solution by ultrafine α-Fe2O3 nanoparticles synthesized from solvent thermal method, J. Hazard. Mater. 192 (2011) 131–138. https://doi.org/10.1016/j.jhazmat.2011.04.111.

[42] Z. Wei, K. Liang, Y. Wu, Y. Zou, J. Zuo, D.C. Arriagada, Z. Pan, G. Hu, The effect of pH on

the adsorption of arsenic(III) and arsenic(V) at the TiO2 anatase [101] surface, J. Colloid Interface Sci. 462 (2016) 252–259. https://doi.org/10.1016/j.jcis.2015.10.018.

[43] J. Giménez, M. Martínez, J. de Pablo, M. Rovira, L. Duro, Arsenic sorption onto natural hematite, magnetite, and goethite, J. Hazard. Mater. 141 (2007) 575–580. https://doi.org/10.1016/j.jhazmat.2006.07.020.

[44] P.K. Dutta, A.K. Ray, V.K. Sharma, F.J. Millero, Adsorption of arsenate and arsenite on titanium dioxide suspensions, J. Colloid Interface Sci. 278 (2004) 270–275. https://doi.org/10.1016/j.jcis.2004.06.015.

[45] N. Deedar, A. Irfan, Q.I. A, Evaluation of the adsorption potential of titanium dioxide nanoparticles for arsenic removal, J. Environ. Sci. 21 (2009) 402–408. https://doi.org/10.1016/S1001-0742(08)62283-4.

[46] G. Morin, Y. Wang, G. Ona-Nguema, F. Juillot, G. Calas, N. Menguy, E. Aubry, J.R. Bargar, G.E. Brown, EXAFS and HRTEM evidence for As(III)-containing surface precipitates on nanocrystalline magnetite: Implications for as sequestration, Langmuir. 25 (2009) 9119–9128. https://doi.org/10.1021/la900655v.

[47] C. Feng, C. Aldrich, J.J. Eksteen, D.W.M. Arrigan, Removal of arsenic from alkaline process waters of gold cyanidation by use of γ-Fe2O3@ZrO2 nanosorbents, Hydrometallurgy. 174 (2017) 71–77. https://doi.org/10.1016/j.hydromet.2017.09.007.

[48] M. Pena, X. Meng, C. Jing, G. Korfiatis, C. Jing, Adsorption Mechanism of Arsenic on Nanocrystalline Titanium Dioxide, (2006) 1257–1262. https://doi.org/10.1021/es052040e.

[49] X. Yang, L. Xia, J. Li, M. Dai, G. Yang, S. Song, Adsorption of As(III) on porous hematite synthesized from goethite concentrate, Chemosphere. 169 (2017) 188–193. https://doi.org/10.1016/j.chemosphere.2016.11.061.

[50] R. Liu, J.F. Liu, L.Q. Zhang, J.F. Sun, G. Bin Jiang, Low temperature synthesized ultrathin γ-Fe2O3 nanosheets show similar adsorption behaviour for As(III) and As(v), J. Mater. Chem. A.

4 (2016) 7606–7614. https://doi.org/10.1039/c6ta01217e.

[51] Y. Li, N. Zhang, J. Chen, R. Li, L. Li, K. Li, Fabrication of α-Fe2O3/TiO2 bi-functional composites with hierarchical and hollow structures and their application in water treatment, J. Nanoparticle Res. 18 (2016) 1–8. https://doi.org/10.1007/s11051-016-3336-y.

[52] A. Maiti, S. DasGupta, J.K. Basu, S. De, Batch and column study: Adsorption of arsenate using untreated laterite as adsorbent, Ind. Eng. Chem. Res. 47 (2008) 1620–1629. https://doi.org/10.1021/ie070908z.

[53] H. Zeng, M. Arashiro, D.E. Giammar, Effects of water chemistry and flow rate on arsenate removal by adsorption to an iron oxide-based sorbent, Water Res. 42 (2008) 4629–4636. https://doi.org/10.1016/j.watres.2008.08.014.

[54] L. Dominguez, J. Economy, K. Benak, C.L. Mangun, Anion exchange fibers for arsenate removal derived from a vinylbenzyl chloride precursor, Polym. Adv. Technol. 14 (2003) 632–637. https://doi.org/10.1002/pat.385.

[55] S. Sarkar, Consumption pattern and determinants of nutritional intake among rural households of West bengal, India, J. Settlements Spat. Plan. 6 (2015) 85–94.

[56] WHO Regional Office for South-East Asia, Minimum water quantity needed for domestic uses, 2005. https://www.google.co.id/?gws_rd=cr&ei=mKloV7G5C8nJ0gSz8Jq4Ag#q=standard+water+consumption+per+person+per+day.

[57] Y. Jia, L. Xu, Z. Fang, G.P. Demopoulos, Observation of surface precipitation of arsenate on ferrihydrite, Environ. Sci. Technol. 40 (2006) 3248–3253. https://doi.org/10.1021/es051872+.

On the application of photocatalyst-sorbent composite materials for arsenic(III) remediation: insights from kinetic adsorption modelling

Supplementary Information

[1*]Jay C. Bullen; [2,3]Chaipat Lapinee; [4]Pascal Salaün; [3]Ramon Vilar and [1*]Dominik J. Weiss

[1]Department of Earth Science and Engineering, Imperial College London, London SW7 2AZ, United Kingdom

[2]Department of Chemistry, School of Science, University of Phayao, Phayao 56000, Thailand

[3]Department of Chemistry, Imperial College London, London SW7 2AZ, United Kingdom

[4]School of Environmental Sciences, University of Liverpool, Liverpool L69 3GP, United Kingdom

*Corresponding author.

Email: j.bullen16@imperial.ac.uk; d.weiss@imperial.ac.uk

1. Further experimental details

1.1. Characterization of TiO_2-Fe_2O_3 bi-functional sorbent

X-ray diffraction (XRD) patterns of the bi-functional sorbent were recorded using an Enraf Nonius PDS 120 X-ray diffractometer using a Co tube 35 kV or 30 mA source, and these patterns used to confirm the Ti and Fe phases in the TiO_2-Fe_2O_3 composite. The particle size-distribution and morphology were examined using a LEO 1455 VP scanning electron microscope (SEM). The BET-specific surface area was calculated from N_2 adsorption-desorption isotherms, determined using a Micromeritics Tristar surface area and Porosity Analyser and Micromeritics FlowPrep 060 Sample Degasser System, using the Brunauer-Emmett-Teller (BET) method.

The point of zero charge was determined by potentiometric titrations using the Metrohm Titrando 888, following a recommended procedure [1]. A 10 g L^{-1} suspension of sorbent in 0.01 M NaCl was acidified with 0.1 M HCl to pH 3 and bubbled with N_2 gas for two hours prior to titration to purge the system of carbonate. A forward titration was carried out with small additions of 0.1 M NaOH to pH 10.5, followed by reverse titration using 0.1 M HCl. Titrations were carried out in 0.05 and 0.1 M NaCl to identify the point of zero salt effect and thus correct for acidic impurities within the sample. Titration curves were converted to profiles of surface charge through the following equation:

$$Q = \frac{(c(acid) - c(base)) - ([H^+] - [OH^-])}{C_s \times SA}$$

Equation 1

where, Q is the surface charge (mol m^{-2}), c(acid) and c(base) are the total concentrations of HCl and NaOH added to the system, $[H^+]$ and $[^-OH]$ were determined by the pH electrode, C_s is the concentration of solid in suspension (g L^{-1}), and SA is the BET-specific surface area of the suspended powder (m^2 g^{-1}).

The isoelectric point was determined by preparing suspensions of the sorbent (1 g L^{-1}) in 0.01 M NaCl and fixing the pH through small additions of 0.01 and 1 M HCl and NaOH, respectively. Suspensions were equilibrated for five days before a final pH reading was taken and the zeta potential measured using a Malvern Zetasizer Nano (3 scans, 6 measurements each).

1.2. Experimental determination of adsorption isotherms and kinetics

Batch adsorption experiments were performed to investigate As(III) adsorption on the TiO_2-Fe_2O_3 bi-functional sorbent in three different buffer solutions at 25 °C (298K): 10 mM KNO_3 (pH 5), 10 mM HEPES (pH 7) and 10 mM borate (pH 9). As(III) concentrations were varied between 20 and 100 mg L^{-1} whilst the sorbent concentration was fixed at 1 g L^{-1}. Suspensions were shaken for 24 hours to achieve equilibrium adsorption. Adsorption kinetics were determined using initial As(III) concentration of 39 mg L^{-1} with 1 g L^{-1} of bi-functional sorbent and 0.01 M KNO_3 in 10 mM HEPES (pH 7) at 25 °C. Aqueous and solid phases were separated by filtration. The sorbent was always in excess of As(III).

1.3. Determination of As(III) using anodic stripping voltammetry

The concentrations of As(III) were measured by square wave anodic stripping voltammetry (SWASV) on a Metrohm 663 VA stand. Solutions were acidified to pH 2 with HCl and purged with N_2 gas prior to analysis. The working, auxiliary and reference electrodes were a 25 µm gold microwire, iridium wire (150 µm diameter, approximately 10 mm long) and a Metrohm glass Ag/AgCl with a KCl (3M) double bridge respectively [2] [3]. The gold microwire electrode was conditioned daily by imposing -3V for 30s in 0.5 M H_2SO_4. Concentrations of As(III) in diluted samples was obtained by the method of standard additions with 2 standard additions and minimum of 3 repeated scans for the blank and additions. Individual SWASV measurements consisted in a conditioning potential of 0.7 V for 3s, followed by the deposition at -1V for 10s, 1s equilibrium time and stripping from -0.2V to 0.1V (using frequency of 50 Hz, amplitude of 50 mV and a step of 6 mV). Quantification of the peak was done after removal of the background current. This latter was obtained by either measuring the background electrolyte in HEPES and acetate (i.e. before dilution of the sample) or by measuring the SWASV signal with a short deposition time of 1s (borate buffer).

1.4. Modelling adsorption isotherms

Langmuir and Freundlich models were used to evaluate adsorption isotherms of As(III) over meso-TiO_2/Fe_2O_3. The Langmuir model assumes that adsorption occurs through formation of a sorbate monolayer across a homogeneous solid surface. Surface active sites are limited and therefore the adsorption reaches a point of saturation at high aqueous sorbate concentrations. The maximum capacity of the Langmuir isotherm is expressed by the following equation:

$$q_e = \frac{Q_{max}\, K_L\, C_e}{1 + K_L\, C_e}$$

Equation 2

where, $C_e$is the equilibrium concentration of As(III) in solution at equilibrium (mg L^{-1}), q_e is the concentration of adsorbed As(III) at equilibrium, i.e. the amount of adsorbed analyte on the solid sorbent, at equilibrium (mg g^{-1} of sorbent), Q_{max} is the maximum adsorption capacity (mg g^{-1} of sorbent) and K_L is the Langmuir constant (L mg^{-1}) [4]. Equation 2 can be re-written in the linear form allowing Q_{max} and K_L to be experimentally derived:

$$\frac{C_e}{q_e} = \frac{1}{K_L\, Q_{max}} + \frac{C_e}{Q_{max}}$$

Equation 3

The Freundlich adsorption model represents multilayer adsorption of sorbate onto the solid surface with Equation 3, and the linear form Equation 4

$$q_e = K_F C_e^{1/n}$$

Equation 4

$$log\, q_e = \frac{1}{n} log\, C_e + log\, K_F$$

Equation 5

where the Freundlich constant, K_F (mg g^{-1} (mg L^{-1}) $^{-1/n}$) and n (dimensionless) are experimentally determined constants [4]. The linear equation of $\log q_e$ as a function of $\log C_e$ is used to test the validity of the model and can be applied to derive K_f and 1/n from the intercept and slope, respectively. These two values are considered relative indicators of adsorption capacity and adsorption intensity, respectively.

1.5. Modelling adsorption kinetics

To assess the rate order and to subsequently determine the overall rate constant, we tested the pseudo first- and pseudo-second order kinetic models. The pseudo-first order model follows the equation:

$$\frac{dq}{dt} = k_1 (q_e - q_t)$$

Equation 6

where q_e is the quantity of arsenic adsorbed at equilibrium (i.e. equivalent to q_e in the adsorption isotherms), q_t is the quantity of arsenic adsorbed at time t (min) and k_1 is the rate constant of the pseudo first order sorption (min^{-1}). The integrated form of Equation 6 can be presented as:

$$log(q_e - q_t) = log\ q_e - \frac{k_1}{2.303}\, t$$

Equation 7

By plotting $\log(q_e - q_t)$ against *t*, the kinetic rate constant (k_1) and adsorption capacity (q_e) were determined.

The pseudo-second order kinetic rate equation is given as:

$$\frac{d_q}{d_t} = k_2 (q_e - q_t)^2$$

Equation 8

where q_e and q_t have the same meaning as above and k_2 is the pseudo-second order rate constant (g mg^{-1} min^{-1}). Equation 8 can be integrated to:

$$\frac{t}{q_t} = \frac{1}{k_2 q_e^2} + \left(\frac{1}{q_e}\right) t$$

Equation 9

By plotting ($\frac{t}{q_t}$) as a function of time t, a linear relationship was obtained and the adsorption capacity q_e and pseudo-second order rate constant, k_2, be calculated from the slope and intercept respectively.

2. Characterisation of the TiO_2-Fe_2O_3 bifunctional sorbent

The XRD pattern of meso-TiO_2/Fe_2O_3 confirmed the presence of crystalline anatase (TiO_2) and hematite (Fe_2O_3) (Figure 1a). A small peak at 32° corresponding to the presence of rutile (TiO_2) as a minority phase was also identified. SEM images showed a wide variety of particle sizes, from sub-micrometre to 40 µm, with sub-spherical shape and a rough/ porous surface structure (Figure 1b). DLS measurements gave a minimum mean particle size of 0.5 µm (pH 9.4) and maximum of 2 µm (pH 7.4). The low maximum particle size observed by DLS may reflect that the larger particles are poorly suspended at pH 7, in 0.01 M NaCl. The BET surface area and pore diameter of the TiO_2 precursor and TiO_2-Fe_2O_3 were 113 and 63 $m^2\ g^{-1}$ respectively with pore diameters of 8.6 and 10.2 nm, respectively, indicating that pores within the TiO_2 powder were filled by Fe_2O_3.

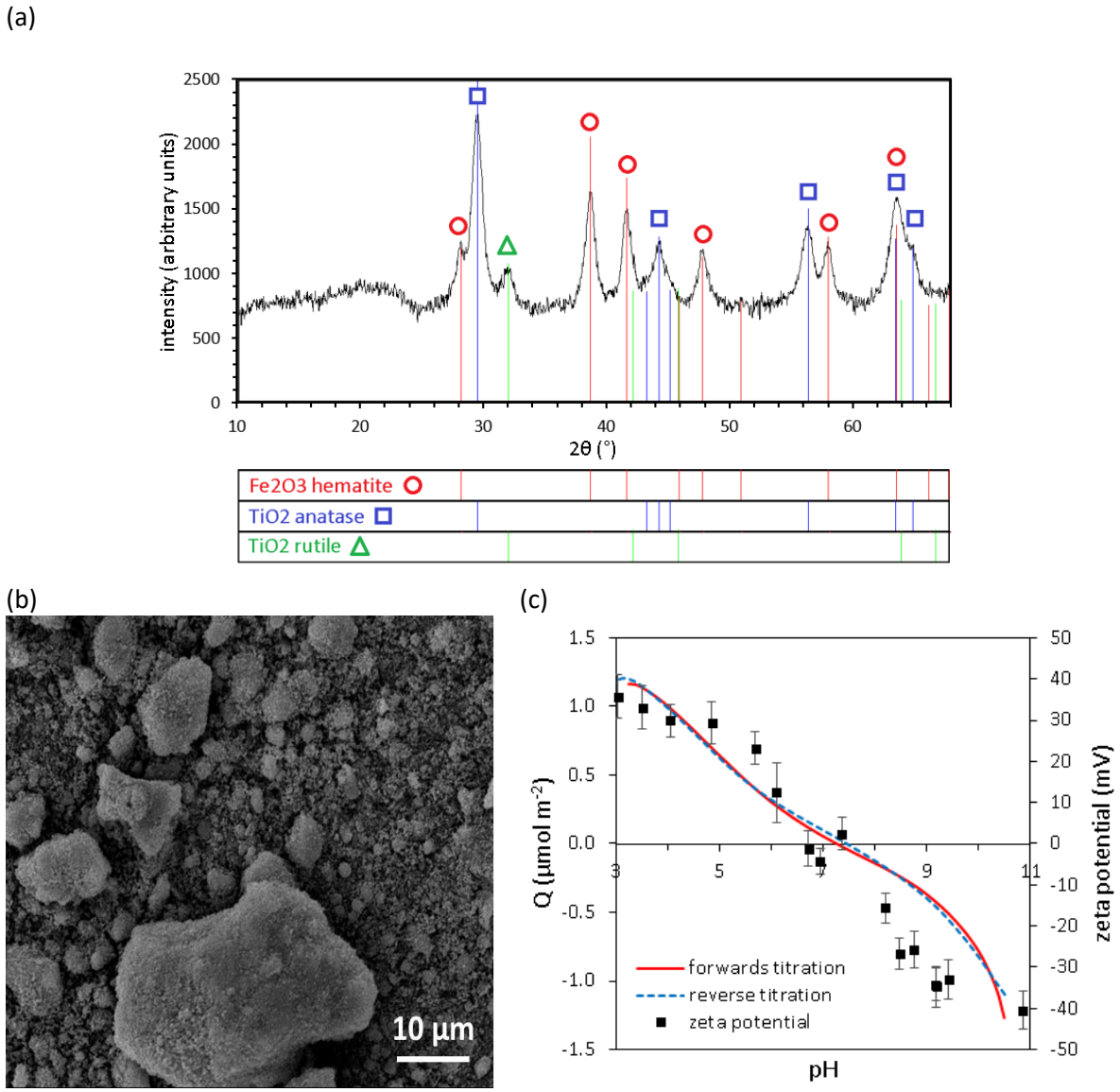

Figure 1: Characterisation of the TiO_2-Fe_2O_3 bi-functional sorbent: (a) XRD pattern; (b) representative SEM image; (c) determination of point of zero charge by potentiometric titration (lines) and zeta potential measurements (squares). Error bars represent the average zeta potential deviation (mV) between the three repeat scans used to determine the average zeta potential (mV) plotted at each point.

Titration curves with surface charge, expressed as the net proton excess, as a function of pH are shown in Figure 1c. We found very good agreement between the point of zero charge when

determined by both potentiometric titration (point of zero salt effect) and zeta potential (isoelectric point). In both cases the pzc was determined to be 7.0 ± 0.2. This lies between the pzc of TiO_2 (pH 5.4-5.9) and Fe_2O_3 (8.3-9.5) [5], indicating that both TiO_2 and Fe_2O_3 phases are exposed on the composite surface. This is potentially advantageous, as both TiO_2 and Fe_2O_3 material components are available for photooxidation and adsorption, respectively.

3. Development of a predictive model

We demonstrated elsewhere that the pseudo-second order model can be modified to give better sensitivity towards changes in C_0 and C_s [6]. To verify that this modified model describes experimental adsorption kinetics with the same quality of fit, we calculated adsorption kinetics with (a) the PSO model but where fixed term q_e replaced with the experimental Freundlich adsorption isotherm, (b) the PSO model but where second order dependence on the **absolute amount** of remaining adsorption capacity replaced with second order dependence on the **relative amount** of remaining adsorption capacity, and (c) the new rate equation, which is a combination of modifications (a) and (b).

Modification (a) was necessary as the PSO parameter q_e is valid only under the specific experimental conditions investigated. The fixed parameter q_e must thus be replaced with a variable adsorption capacity that is a function of C_0 and C_s. This is best achieved by using an adsorption isotherm to calculate the parameter at each time point, and is in fact recommended by Huang et al., to give a better account of the driving force of adsorption in the initial stages of reaction [7]. C_t was used in place of C_e in the Freundlich adsorption isotherm expression as (i) we do not know what C_e will be in in a batch reaction without a considerably more complex expression (ii) the system itself does not know what C_e will be in the future, it only knows what C_t is right now, and (iii) for a continuous flow system C_e is not a meaningful concept, as the system is in a continual state of disequilibrium. The value used for q_e therefore ceases to be the equilibrium concentration of adsorbed sorbate, and the subscript 'e' character should not be taken to mean 'equilibrium'. The rate equation takes the form:

$$\frac{dq_t}{d_t} = k_2 \left(K_F {C_t}^{1/n} - q_t \right)^2$$

Equation 10: PSO equation with Freundlich adsorption isotherm modification

Under the initial conditions (30 mg L^{-1} As(III) (aq), 1 g L^{-1} sorbent, q_e = 17 mg L^{-1}), the new expression is not entirely mathematically equivalent, as at time t=0, C_t is greater than C_e (sorbate concentration at equilibrium). Therefore, the value of q_e calculated using the Freundlich adsorption isotherm is greater at t=0 than at equilibrium, giving rise to slightly faster kinetic rates at the start of reaction (Figure 2a, 'PSO (Freundlich)'). Despite the Freundlich adsorption isotherm returning a higher value of 'q_e' at the start of the reaction leading to an increased rate of adsorption, we indeed observed that incorporation of the Freundlich adsorption isotherm into the pseudo-second order equation gave a fit to the experimental data no worse than when q_e was fixed. This new rate equation very closely approximates the original pseudo-second order rate equation, albeit with faster initial kinetics owing to the high value of q_e returned by the Freundlich adsorption isotherm at the initial stages of reaction. Despite the difference, the goodness of fit to the experimental data was slightly improved. Huang et al. suggest that this actually gives a better account of the driving force of the reaction at early points in time [7].

Modification (b) is necessary to remove the conditionality that the PSO rate constant k_2 shows towards changes in C_0 (k_2 is approximately inversely proportional to C_0). This modification results in the following rate equation:

$$\frac{dq}{d_t} = k' \left(1 - \frac{q_t}{q_e} \right)^2$$

Equation 11: PSO with second order dependence on relative concentration of available surface, rather than the absolute concentration of available surface

where $k' = k_2 {q_e}^{\dagger 2}$ with $q_e^{\dagger}$ denoting the equilibrium concentration of adsorbed sorbate in the particular kinetic experiment used to calculate k_2. Modification of the equation to this form, with second order dependence on the **relative** concentration of unused adsorption capacity rather than the **absolute** concentration, results in no significant difference in the goodness of fit (Figure 2a, 'PSO (relative)').

The final form of our modified rate equation was $\frac{dq}{d_t} = k' C_t \left(1 - \frac{q_t}{q_e}\right)^2$, giving the first order dependence of rate upon sorbate concentration that is typically seen experimentally in the literature [6]. In this model $k' = \frac{k_2 {q_e}^{\dagger 2}}{{C_0}^{\dagger}}$ where $C_0^{\dagger}$ denotes the initial sorbate concentration in the particular kinetic experiment used to calculate k_2. The original PSO model has no sensitivity towards C_0 and C_s. The new kinetic model is first order towards C_t and incorporates sensitivity to C_s through the adsorption isotherm determination of q_e. Despite these differences the modified model faithfully reconstructed the adsorption kinetics in the original PSO from which it was derived. The modified model is labelled "PSO (final)" in Figure 2b. We thus demonstrate that whilst providing sensitivity towards changes in C_0 and C_s that were lacking in the original PSO, the modified rate equation successfully reduces to the original PSO when under the same conditions.

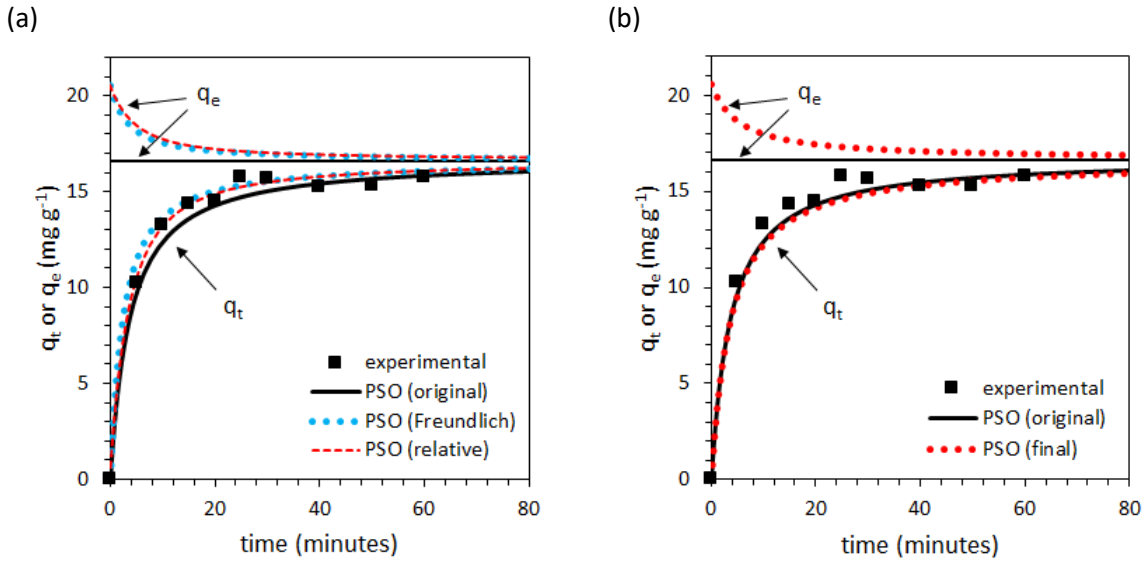

Figure 2: Comparison of modified adsorption kinetic models with the unmodified PSO. (a) Comparison of original PSO model with (i) Freundlich modification, and (ii) modification to second order dependence on the relative amount of remaining adsorption capacity. (b) comparison of the original pseudo-second order model with the final modified model. The labels 'q_t' and 'q_e' indicate the quantity of adsorbed As(III) and the fixed or calculated value of q_e at each time point respectively. Note that the magnitude of the Freundlich constant K_F has been increased (from 4.06 to 5.10) to account for the 26% difference in q_e observed between the adsorption isotherm and kinetic experiments when C_e = 22.5 mg L^{-1} (in the Freundlich adsorption isotherm when C_e = 22.4 mg L^{-1}, q_e = 13.3 mg g^{-1}, in the kinetic experiments when C_e = 22.4 mg L^{-1}, q_e = 16.7 mg g^{-1}).
The four models presented are labelled as follows: PSO (original): $\frac{dq_t}{d_t} = k_2(q_e - q_t)^2$, PSO (Freundlich): $\frac{dq_t}{d_t} = k_2(K_F {C_t}^{1/n} - q_t)^2$, PSO (relative): $\frac{dq_t}{d_t} = k'(1 - \frac{q_t}{K_F {C_t}^{1/n}})^2$ where $k' = k_2 {q_e}^{\dagger 2}$, PSO (final): $\frac{dq}{d_t} = k' C_t (1 - \frac{q_t}{q_e})^2$ where $k' = \frac{k_2 {q_e}^{\dagger 2}}{C_{0*}}$.

4. Further simulated results

4.1.1. Sorbent efficiency (mg g^{-1} adsorbed at end of year or breakthrough)

Sorbent efficiency (mg g^{-1} adsorbed at the end of 365 days or at breakthrough, whichever occurs soonest). The initial As(III) concentration was 500 µg L^{-1}.

(a) Batch treatment

batch treatment time (min) \ sorbent loading (g L^{-1})	0.01	0.1	1	10	100	1000	10000
1	0.00	0.00	0.00	0.00	0.50	0.18	0.02
2	0.00	0.00	0.00	0.00	0.75	0.18	0.02
5	0.00	0.00	0.00	0.25	0.75	0.18	0.02
10	0.00	0.00	0.00	0.50	0.75	0.18	0.02
20	0.00	0.00	0.00	0.75	0.88	0.18	0.02
50	0.00	0.00	0.00	0.75	0.88	0.18	0.02
100	0.00	0.00	0.50	0.85	0.88	0.18	0.02
200	0.00	0.00	0.50	0.85	0.88	0.18	0.02
500	0.00	0.00	0.50	0.85	0.88	0.18	0.02
1000	0.00	0.00	0.50	0.85	0.89	0.18	0.02

(b) Continuous-flow treatment

average residence time (min) \ sorbent loading (g L^{-1})	0.01	0.1	1	10	100	1000	10000
1	0.00	0.00	0.00	0.00	0.00	0.83	0.87
2	0.00	0.00	0.00	0.00	0.00	0.47	0.76
5	0.00	0.00	0.00	0.00	0.06	0.63	0.81
10	0.00	0.00	0.00	0.00	0.30	0.70	0.83
20	0.00	0.00	0.00	0.00	0.47	0.76	0.85
50	0.00	0.00	0.00	0.06	0.63	0.81	0.53
100	0.00	0.00	0.01	0.30	0.70	0.83	0.26
200	0.00	0.00	0.01	0.47	0.76	0.85	0.13
500	0.00	0.00	0.07	0.63	0.81	0.53	0.05
1000	0.00	0.00	0.32	0.70	0.83	0.26	0.03

4.1.2. Mass of sorbent required per household per year – Ratio of continuous flow reactor/batch reactor

The ratio between the mass of sorbent needed to treat water contaminated with 500 µg L^{-1} As(III). Blank cells indicate conditions under which the continuous-flow models was unable to provide at least 1 day of safe water (<10 µg L^{-1} As(III)).

batch treatment time (min) \ sorbent loading (g L^{-1})	0.01	0.1	1	10	100	1000	10000
1	-	-	-	-	-	0.22	0.02
2	-	-	-	-	-	0.38	0.02
5	-	-	-	288.35	13.61	0.29	0.02
10	-	-	-	455.37	2.49	0.26	0.02
20	-	-	-	561.80	1.84	0.24	0.02
50	-	-	-	13.20	1.40	0.23	0.03
100	-	-	44.88	2.80	1.24	0.22	0.07
200	-	-	37.65	1.79	1.16	0.21	0.14
500	-	-	6.78	1.35	1.09	0.35	0.35
1000	-	-	1.57	1.21	1.07	0.69	0.69

5. MATLAB codes

MATLAB codes used to simulate the arsenic treat models (batch and continuous-flow) are presented here, and are also available at http://doi.org/10.5281/zenodo.3690170 [8].

5.1. Simulating a single batch treatment

```
%This code runs a two-dimensional matrix of separate kinetic experiments,
%each experiment with a unique combination of sorbent concentration (Cs)
%and initial sorbate concentration (C0).

%Adsorption kinetics are modelled using the modified pseudo-second order
%rate equation, being (a) second order with respect to the relative
%proportion of adsorption capacity remaining (with maximum adsorption
%capacity determined using the Freundlich adsorption isotherm), (b) first
%order with respect to sorbate concentration, and (c) zero-/first- order
%with respect to sorbent concentration when the rate is normalised to
%sorbent concentration and total volume, respectively.%

function main

%this section of code tells MATLAB to run the kinetic model with a
%different value for the sorent concentration, Cs, each time
run('batch_001.txt',0.01);
run('batch_002.txt',0.02);
run('batch_005.txt',0.05);
run('batch_01.txt',0.1);
run('batch_02.txt',0.2);
run('batch_05.txt',0.5);
run('batch_1.txt',1.0);
run('batch_2.txt',2);
run('batch_5.txt',5);
run('batch_10.txt',10);
run('batch_20.txt',20);
run('batch_50.txt',50);
run('batch_100.txt',100);
```

```
run('batch_200.txt',200);

run('batch_500.txt',500);

run('batch_1000.txt',1000);


end



function run(filename,Cs0)

number_of_experiments=54; %each experiment will have a different initial sorbate
concentration (C0)

number_of_variables = 8; %counting how many rows in the array we need to store the
input parameters for each kinetic plot


experiments = zeros(number_of_experiments,number_of_variables);   %each experiment
refers to a single kinetic plot

%creating the input variables for each kinetic plots

C_init = 0;     %ppb or ug L-1 - this is the initial concentration of aqueous
sorbate in the ssuspension

q_init = 0;     %ppb or ug L-1 - this is the initial concentration of adsorbed
sorbate in the suspension

Cs = Cs0;       %g L-1 - this is the concentration of sorbent

Cinfluent = 0;  %ppb or ug L-1 - this is the concentration of sorbate in the
influent (for continuous-flow modelling)

j = 0;          %this the turn-over frequency, i.e. bed volumes per minute

k = 0.1111;     %this is the value of normalised k' (L g-1 min-1)

KF = 5.10;      %this is the Freundlich constant (mg g-1) used to determine 'qe' at
each time step

n = 2.63;       %this is the second parameter for the Freundlich adsorption
isotherm (g L-1) used to determine 'qe' at each time step


%setting the time intervals upon which data is recorded

t_end = 4320;   %1440 = 1 day

t_steps = 2000;

t_step = t_end/t_steps;

bv_end = t_end*j;


%setting up the arrays where calculated data is to be stored

global results_t;

results_t = zeros(number_of_experiments,t_steps+1);

global results_Ct;
```

```
results_Ct = zeros(number_of_experiments,t_steps+1);
global results_qt;
results_qt = zeros(number_of_experiments,t_steps+1);
global exp;


%we make an array listing all the input parameters for each kinetic plot we
%wish to model. The different values of Cs are automatically plugged in
for i = 1:number_of_experiments
    experiments(i,1) = C_init;
    experiments(i,2) = q_init;
    experiments(i,3) = j;
    experiments(i,4) = Cinfluent;
    experiments(i,5) = k;
    experiments(i,6) = Cs;
    experiments(i,7) = KF;
    experiments(i,8) = n;
end

%here we overwrite the initial aqueous sorbate concentration, C0, with a
%concentration ranging from 10 ug L-1 to 2000 ug L-1, representing the
%arsenic levels in natural water that we are interested in treating
experiments(1,1) = 10;
experiments(2,1) = 20;
experiments(3,1) = 40;
experiments(4,1) = 60;
experiments(5,1) = 80;
experiments(6,1) = 100;
experiments(7,1) = 125;
experiments(8,1) = 150;
experiments(9,1) = 175;
for i=10:46
experiments(i,1) = ((i-9)*50)+150;
end
for i=47:number_of_experiments
experiments(i,1) = ((i-46)*500)+2000;
end
```

```
%setting up the formatting for printing results

results_table=[];

formatSpec = '';

formatSpec2 = '';

formatHeader = '';


 for i = 1:number_of_experiments

exp = zeros(1,number_of_variables) ;

exp(1,:) = experiments(i,:);


exp_C_init = exp(1,1);

exp_q_init = exp(1,2);


%run the ode45 function which will solve the differential rate equation

[t,C]=ode45(@DiffEq,[0:t_step:t_end],[exp_C_init exp_q_init]);   %call the ODE
function


results_t(i,:) = t;

results_bv(i,:) = results_t(i,:)*exp(1,3);

results_Ct(i,:) = C(:,1);

results_qt(i,:) = C(:,2);

results_theta(i,:) = C(:,2)/(1000*exp(1,7));


results_table =
[results_table,results_t(i,:).',results_bv(i,:).',results_Ct(i,:).',results_qt(i,:)
.',results_theta(i,:).']


%print the results

%formatSpec = strcat(formatSpec,'\r\n')

fileID = fopen(filename,'w');

%formatSpec = '%10.3f %10.5f %10.3f %10.3f %10.8f\r\n';

%fprintf(fileID,'%10s %10s %10s %10s %10s %10s %10s\r\n,'C0,ppb','q0,ppb','j,BV
min-1','C_inf,ppb','k','Cs,g L-1','qm,mg g-1');

%formatHeader = strcat(formatHeader,'\r\n');


formatHeader = '';

for i = 1:number_of_experiments
```

```
formatHeader = strcat(formatHeader,'%-50.4f ');
end
%formatHeader = strcat(formatHeader,'%-50.4f ');
fprintf(fileID,strcat(formatHeader,'\r\n'),experiments(:,:));
formatSpec2 = strcat(formatSpec2,'%10s %10s %10s %10s %10s\r\n');
fprintf(fileID,formatSpec2,'t','BV','Ct','qt','theta');
%formatSpec = strcat(formatSpec,'%10.3f %10.5f %10.3f %10.3f %10.8f');
formatSpec = strcat(formatSpec,'%.5E %.5E %.5E %.5E %.5E');
fprintf(fileID,strcat(formatSpec,'\r\n'),results_table.');
fclose(fileID);

end

end

function dCdt = DiffEq(t,conditions)
global exp;

time=t;

j = exp(1,3);
Cinfluent = exp(1,4);
k = exp(1,5);
Cs = exp(1,6);
KF = exp(1,7);
n = exp(1,8);

Ct = conditions(1);   %ppb
qt = conditions(2);   %ppb
Ct_mgL = Ct/1000;         %mg L-1
qt_mgg = qt/(Cs*1000);    %mg g-1

%the rate equation we are using is
%dqt/dt = k' * Ct * (1-(qt/(Kf * Ce^(1/n))))^2
%please see our manuscript for derivation and further information
```

```
rate_ads = 1000*k*Ct_mgL*Cs*((1-(qt_mgg/(KF*(Ct_mgL^(1/n)))))^2); %calculate dq/dt
in ppb L-1 min-1

rate_influx = j*Cinfluent; %calculate the rate of sorbate influx (continuous-flow
systems only)

rate_outflux = j*Ct; %calculate the rate of sorbate outflux (continuous-flow
systems only)

dCdt = [-rate_ads+rate_influx-rate_outflux;rate_ads]; %adjust the concentration of
aqueous sorbate and adsorbed sorbate, respectively

end
```

5.2. Simulating continuous-flow

```
%This code runs a series of kinetic models in a continuous-flow simulation.


%Adsorption kinetics are modelled using the modified pseudo-second order

%rate equation, being (a) second order with respect to the relative

%proportion of adsorption capacity remaining (with maximum adsorption

%capacity determined using the Freundlich adsorption isotherm), (b) first

%order with respect to sorbate concentration, and (c) zero-/first- order

%with respect to sorbent concentration when the rate is normalised to

%sorbent concentration and total volume, respectively.%


function main


%this section of code tells MATLAB to run the kinetic model with a

%unique combinations of sorbent concentration, flow rate, and initial sorbate

%concentrations. The high sorbent concentration models are run last, as

%these are the most computationally demanding simulations.

run('data3.txt',5,0.01,500,0.01);

run('data4.txt',5,0.02,500,0.01);

run('data5.txt',5,0.05,500,0.01);

run('data6.txt',5,0.1,500,0.01);

run('data7.txt',5,0.2,500,0.01);

run('data8.txt',5,0.5,500,0.01);

run('data9.txt',5,1.0,500,0.01);


run('data10.txt',5,0.01,2000,0.01);

run('data11.txt',5,0.02,2000,0.01);
```

```
run('data12.txt',5,0.05,2000,0.01);
run('data13.txt',5,0.1,2000,0.01);
run('data14.txt',5,0.2,2000,0.01);
run('data15.txt',5,0.5,2000,0.01);
run('data16.txt',5,1.0,2000,0.01);

run('data17.txt',5,0.01,1000,0.01);
run('data18.txt',5,0.02,1000,0.01);
run('data19.txt',5,0.05,1000,0.01);
run('data20.txt',5,0.1,1000,0.01);
run('data21.txt',5,0.2,1000,0.01);
run('data22.txt',5,0.5,1000,0.01);
run('data23.txt',5,1.0,1000,0.01);

run('data24.txt',1,0.01,500,1000);
run('data25.txt',1,0.02,500,1000);
run('data26.txt',1,0.05,500,1000);
run('data27.txt',1,0.1,500,1000);
run('data28.txt',1,0.2,500,1000);
run('data29.txt',1,0.5,500,1000);
run('data30.txt',1,1.0,500,1000);

run('data31.txt',1,0.01,2000,1000);
run('data32.txt',1,0.02,2000,1000);
run('data33.txt',1,0.05,2000,1000);
run('data34.txt',1,0.1,2000,1000);
run('data35.txt',1,0.2,2000,1000);
run('data36.txt',1,0.5,2000,1000);
run('data37.txt',1,1.0,2000,1000);

run('data38.txt',1,0.01,1000,1000);
run('data39.txt',1,0.02,1000,1000);
run('data40.txt',1,0.05,1000,1000);
run('data41.txt',1,0.1,1000,1000);
run('data42.txt',1,0.2,1000,1000);
run('data43.txt',1,0.5,1000,1000);
run('data44.txt',1,1.0,1000,1000);
```

```
run('data45.txt',1,0.01,500,10000);
run('data52.txt',1,0.01,2000,10000);
run('data48.txt',1,0.1,500,10000);
run('data55.txt',1,0.1,2000,10000);
run('data51.txt',1,1.0,500,10000);
run('data58.txt',1,1.0,2000,10000);
run('data59.txt',1,0.01,1000,10000);
run('data62.txt',1,0.1,1000,10000);
run('data65.txt',1,1.0,1000,10000);

run('data46.txt',1,0.02,500,10000);
run('data47.txt',1,0.05,500,10000);

run('data49.txt',1,0.2,500,10000);
run('data50.txt',1,0.5,500,10000);

run('data53.txt',1,0.02,2000,10000);
run('data54.txt',1,0.05,2000,10000);

run('data56.txt',1,0.2,2000,10000);
run('data57.txt',1,0.5,2000,10000);

run('data60.txt',1,0.02,1000,10000);
run('data61.txt',1,0.05,1000,10000);

run('data63.txt',1,0.2,1000,10000);
run('data64.txt',1,0.5,1000,10000);

run('data66.txt',5,0.001,500,0.01);
run('data67.txt',5,0.002,500,0.01);
run('data68.txt',5,0.005,500,0.01);
run('data69.txt',5,0.001,2000,0.01);
run('data70.txt',5,0.002,2000,0.01);
run('data71.txt',5,0.005,2000,0.01);
run('data72.txt',5,0.001,1000,0.01);
run('data73.txt',5,0.002,1000,0.01);
```

```
run('data74.txt',5,0.005,1000,0.01);


run('data75.txt',1,0.001,500,1000);

run('data76.txt',1,0.002,500,1000);

run('data77.txt',1,0.005,500,1000);

run('data78.txt',1,0.001,2000,1000);

run('data79.txt',1,0.002,2000,1000);

run('data80.txt',1,0.005,2000,1000);

run('data81.txt',1,0.001,1000,1000);

run('data82.txt',1,0.002,1000,1000);

run('data83.txt',1,0.005,1000,1000);


run('data84.txt',1,0.001,500,10000);

run('data87.txt',1,0.001,2000,10000);

run('data90.txt',1,0.001,1000,10000);


run('data85.txt',1,0.002,500,10000);

run('data86.txt',1,0.005,500,10000);

run('data88.txt',1,0.002,2000,10000);

run('data89.txt',1,0.005,2000,10000);

run('data91.txt',1,0.002,1000,10000);

run('data92.txt',1,0.005,1000,10000);


end



function run(filename,number_exps,j_flow,C_inf,Cs0)

number_of_experiments=number_exps;  %each experiment will have a different initial
sorbate concentration (C0)

number_of_variables = 8;            %counting how many rows in the array we need to
store the input parameters for each kinetic plot


experiments = zeros(number_of_experiments,number_of_variables);   %each experiment
refers to a single kinetic plot

%creating the input variables for each kientic plots

C_init = 0.001;     %ppb or ug L-1 - this is the initial concentration of aqueous
sorbate in the ssuspension

q_init = 0;     %ppb or ug L-1 - this is the initial concentration of adsorbed
sorbate in the suspension
```

```
Cs = Cs0;       %g L-1 - this is the concentration of sorbent

Cinfluent = C_inf;  %ppb or ug L-1 - this is the concentration of sorbate in the
influent (for continuous-flow modelling)

j = j_flow;          %this the turn-over frequency, i.e. bed volumes per minute

k = 0.1111;     %this is the value of normalised k' (L g-1 min-1)

KF = 5.10;      %this is the Freundlich constant (mg g-1) used to determine 'qe' at
each time step

n = 2.63;       %this is the second parameter for the Freundlich adsorption
isotherm (g L-1) used to determine 'qe' at each time step


%setting the time intervals upon which data is recorded. This will be

%overwritten later to avoid wasting computational time after breakthrough

%has already occurred.

t_end = 1000000;   %1440 = 1 day

t_steps = 2000;

t_step = t_end/t_steps;

bv_end = t_end*j;


%setting up the arrays where calculated data is to be stored

global results_t;

results_t = zeros(number_of_experiments,t_steps+1);

global results_Ct;

results_Ct = zeros(number_of_experiments,t_steps+1);

global results_qt;

results_qt = zeros(number_of_experiments,t_steps+1);

global exp;


%we make an array listing all the input parameters for each kinetic plot we

%wish to model. The different values of Cs are automatically plugged in

for i = 1:number_of_experiments

    experiments(i,1) = C_init;

    experiments(i,2) = q_init;

    experiments(i,3) = j;

    experiments(i,4) = Cinfluent;

    experiments(i,5) = k;

    experiments(i,6) = Cs*10^(i-1); %exponentially increasing sorbent concentration

    experiments(i,7) = KF;

    experiments(i,8) = n;
```

```
end

%setting up the formatting for printing results
results_table=[];
formatSpec = '';
formatSpec2 = '';
formatHeader = '';

%for i = 1:1number_of_experiments
for i = 1:number_of_experiments
exp = zeros(1,number_of_variables);
exp(1,:) = experiments(i,:);
exp_C_init = exp(1,1);
exp_q_init = exp(1,2);

%making sure that we model an appropriate length of time (duration) with
%appropriate interval lengths for each simulation.
%t_end = 9100 * exp(1,6) / (exp(1,3) * exp(1,4));  % 50000*Cs/(j*Cinf)
t_end = 12000 * exp(1,6) / (exp(1,3) * exp(1,4));  % 50000*Cs/(j*Cinf)
 if t_end<1000
     t_end = t_end*20;
 end
 if t_end<500
     t_end=t_end*5;
 end
 if j<0.01
     t_end=t_end*10;
 end
%t_step = t_end/t_steps;
stepping = [1:1:t_steps+1];      %collect data at shorter time intervals in the
initial stages of the simulation
stepping(1)=0;
gradient_1=1;
gradient_2=60;
for i = 2:(t_steps+1)
    %change the time intervals from being evenly spaced to having a smooth
    %transition from gradient_1 to gradient_2
```

```
    stepping(i)=stepping(i-
1)+(gradient_2*(stepping(i)/t_steps))+(gradient_1*((t_steps-stepping(i))/t_steps));

end

for i = 2:(t_steps+1)

    %normalise the time intervals to 1 and then multiply out by the desired

    %final time

    stepping(i)=(stepping(i)/stepping(t_steps+1))*t_end;

    %"i is " + i +" and stepping(i) is " + stepping(i)

end


% %speed up ode15s for simulations with 1000+ g L-1 for shorter processing times

% global speed;

% speed=1

% if exp(1,6)>100

%     speed=exp(1,6)/100

% end

% [stepping]=[stepping]/speed; %and replace the time steps to be recorded by re-
scaled time intervals


%run the ode15s function which will solve the differential rate equation

options = odeset('RelTol',1e-4,'Stats','on','OutputFcn',@odeplot);   %need to
increase the tolerance to avoid errors, was 1e-5 to begin with, tried changing to
1e-4

[t,C]=ode15s(@DiffEq,[stepping],[exp_C_init exp_q_init],options);   %call the ODE
function

%[t,C]=ode15s(@DiffEq,[stepping],[exp_C_init exp_q_init]);   %call the ODE function

%[t,C]=ode15s(@DiffEq,[0:t_step:t_end],[exp_C_init exp_q_init]);   %call the

%ODE function - original call with equal spacing between time intervals


results_t(i,:) = t;

%results_t(i,:) = t/speed;

results_bv(i,:) = results_t(i,:)*exp(1,3);

results_Ct(i,:) = C(:,1);

results_qt(i,:) = C(:,2);

results_theta(i,:) = C(:,2); %ignore, we are not calculating theta


results_table =
[results_table,results_t(i,:).',results_bv(i,:).',results_Ct(i,:).',results_qt(i,:)
.',results_theta(i,:).']
```

```
%print the results

%formatSpec = strcat(formatSpec,'\r\n')

fileID = fopen(filename,'w');

%formatSpec = '%10.3f %10.5f %10.3f %10.3f %10.8f\r\n';

%fprintf(fileID,'%10s %10s %10s %10s %10s %10s %10s\r\n,'C0,ppb','q0,ppb','j,BV
min-1','C_inf,ppb','k','Cs,g L-1','qm,mg g-1');

%formatHeader = strcat(formatHeader,'\r\n');


formatHeader = '';

for i = 1:number_of_experiments

formatHeader = strcat(formatHeader,'%-50.4f ');

end

%formatHeader = strcat(formatHeader,'%-50.4f ');

fprintf(fileID,strcat(formatHeader,'\r\n'),experiments(:,:));

formatSpec2 = strcat(formatSpec2,'%14s %14s %14s %14s %14s\r\n');

fprintf(fileID,formatSpec2,'t','BV','Ct','qt','theta');

%formatSpec = strcat(formatSpec,'%10.3f %10.5f %10.3f %10.3f %1.0f');

formatSpec = strcat(formatSpec,'% 0.3E % 0.3E % 0.3E % 0.3E % 0.3E');

%formatSpec = strcat(formatSpec,'%0.3E %0.3E %0.3E %0.3E %0.3E ');

%formatSpec = strcat(formatSpec,'%.5E %.5E %.5E %.5E %.5E');

fprintf(fileID,strcat(formatSpec,'\r\n'),results_table.',' %s');

fclose(fileID);


"just completed simulation with: j = " + j_flow + " and C_inf = " + C_inf


end


"just completed file: " + filename


end


function dCdt = DiffEq(t,conditions)

global exp;

%global speed


time=t;
```

```
j = exp(1,3);

Cinfluent = exp(1,4);

k = exp(1,5);

Cs = exp(1,6);

KF = exp(1,7);

n = exp(1,8);


Ct = conditions(1);   %ppb

if Ct<0.001

   Ct=0.001;            %set a minimum concentration of sorbate in the reactor to
prevent the Freundlich adsorption isotherm from running an error.

end

if Ct>Cinfluent

    Ct=Cinfluent;       %control incase ode15s time intervals are too large

end

qt = conditions(2);   %ppb

Ct_mgL = Ct/1000;         %mg L-1

qt_mgg = qt/(Cs*1000);    %mg g-1


"Ct is " + Ct + " ug L-1 and qt is " + qt + "ug L-1"


%the rate equation we are using is

%dqt/dt = k' * Ct * (1-(qt/(Kf * Ce^(1/n))))^2

%please see our manuscript for derivation and further information


rate_ads = 1000*k*Ct_mgL*Cs*((1-(qt_mgg/(KF*(Ct_mgL^(1/n))))))^2); %calculate dq/dt
in ppb L-1 min-1

rate_influx = j*Cinfluent; %calculate the rate of sorbate influx (continuous-flow
systems only)

rate_outflux = j*Ct; %calculate the rate of sorbate outflux (continuous-flow
systems only)


dCdt = [-rate_ads+rate_influx-rate_outflux;rate_ads]; %adjust the concentration of
aqueous sorbate and adsorbed sorbate, respectively

%dCdt = [speed*(-rate_ads+rate_influx-rate_outflux);speed*(rate_ads)]; %adjust the
concentration of aqueous sorbate and adsorbed sorbate, respectively

end
```

5.3. Simulating 365 days sequential batch treatment

```
%This code runs a batch adsorption model, 365 days, representing a single
%mass of sorbent being used for 365 consecutively

%Adsorption kinetics are modelled using the modified pseudo-second order
%rate equation, being (a) second order with respect to the relative
%proportion of adsorption capacity remaining (with maximum adsorption
%capacity determined using the Freundlich adsorption isotherm), (b) first
%order with respect to sorbate concentration, and (c) zero-/first- order
%with respect to sorbent concentration when the rate is normalised to
%sorbent concentration and total volume, respectively.%
function main
global day;
global qt;              %variable qt will keep track of how much sorbate is
attached to the sorbent at the end of each day
qt = [0 0 0 0 0 0 0];
for day = 1:365
run(strcat('500ppb_day_',sprintf('%03d',day),'.txt'),500,10,qt);     %for 365 days,
run the experiment
end
qt = [0 0 0 0 0 0 0];
for day = 1:365
run(strcat('2000ppb_day_',sprintf('%03d',day),'.txt'),2000,10,qt);     %for 365
days, run the experiment
end


end



function run(filename,C0,Cs0,qt)
global qt;
global i;
number_of_experiments=7;
number_of_variables = 8;

experiments = zeros(number_of_experiments,number_of_variables);
```

```
C_init = C0;     %ppb or ug L-1 - this is the initial concentration of aqueous
sorbate in the ssuspension

q_init = qt;     %ppb or ug L-1 - this is the initial concentration of adsorbed
sorbate in the suspension

Cs = Cs0;        %g L-1 - this is the concentration of sorbent

Cinfluent = 0;  %ppb or ug L-1 - this is the concentration of sorbate in the
influent (for continuous-flow modelling)

j = 0;           %this the turn-over frequency, i.e. bed volumes per minute

k = 0.1111;      %this is the value of normalised k' (L g-1 min-1)

KF = 5.10;       %this is the Freundlich constant (mg g-1) used to determine 'qe' at
each time step

n = 2.63;        %this is the second parameter for the Freundlich adsorption
isotherm (g L-1) used to determine 'qe' at each time step


data_collect = [0   1     2     3     4     5     6     7     8     9     10
      20    30    40    50    60    70    80    90    100   110   120   150
      180   210   240   270   300   330   360   390   420   450   480   510
      540   570   600   630   660   690   720   750   780   810   840   870
      900   930   960   990   1020  1050  1080  1110  1140  1170  1200
      1230  1260  1290  1320  1350  1380  1410  1440

];

t_end = 1440; %1440 = 1 day

t_steps = numel(data_collect);

%t_step = t_end/t_steps;

bv_end = t_end*j;


%setting up the arrays where calculated data is to be stored

global results_t;

results_t = zeros(number_of_experiments,t_steps);

global results_Ct;

results_Ct = zeros(number_of_experiments,t_steps);

global results_qt;

results_qt = zeros(number_of_experiments,t_steps);

global exp;


%we make an array listing all the input parameters for each kinetic plot we

%wish to model. The different values of Cs are automatically plugged in

for i = 1:number_of_experiments

    experiments(i,1) = C_init;

    experiments(i,2) = qt(i);

    experiments(i,3) = j;
```

```
    experiments(i,4) = Cinfluent;
    experiments(i,5) = k;
    experiments(i,6) = Cs *10^(i-4); %10^(i-2);
    experiments(i,7) = KF;
    experiments(i,8) = n;
end

%setting up the formatting for printing results
results_table=[];
formatSpec = '';
formatSpec2 = '';
formatHeader = '';

for i = 1:number_of_experiments
exp = zeros(1,number_of_variables) ;
exp(1,:) = experiments(i,:);
exp_C_init = exp(1,1);
exp_q_init = exp(1,2);

%increase the tolerance
options = odeset('RelTol',1e-3);   %need to increase the tolerance to avoid errors,
was 1e-5 to begin with, tried changing to 1e-4
%run the ode45 function which will solve the differential rate equation
[t,C]=ode45(@DiffEq,[data_collect],[exp_C_init exp_q_init]);   %call the ODE
function

results_t(i,:) = t;
results_bv(i,:) = results_t(i,:)*exp(1,3);
results_Ct(i,:) = C(:,1);
results_qt(i,:) = C(:,2);
results_theta(i,:) = C(:,2)/(1000*exp(1,7));   %now meaningless

results_table =
[results_table,results_t(i,:).',results_bv(i,:).',results_Ct(i,:).',results_qt(i,:)
.',results_theta(i,:).']

%print here
```

```
%formatSpec = strcat(formatSpec,'\r\n')

fileID = fopen(filename,'w');

%formatSpec = '%10.3f %10.5f %10.3f %10.3f %10.8f\r\n';

%fprintf(fileID,'%10s %10s %10s %10s %10s %10s %10s\r\n,'C0,ppb','q0,ppb','j,BV
min-1','C_inf,ppb','k','Cs,g L-1','qm,mg g-1');

%formatHeader = strcat(formatHeader,'\r\n');


formatHeader = '';

for i = 1:number_of_experiments

formatHeader = strcat(formatHeader,'%-50.4f ');

end

%formatHeader = strcat(formatHeader,'%-50.4f ');

fprintf(fileID,strcat(formatHeader,'\r\n'),experiments(:,:));

formatSpec2 = strcat(formatSpec2,'%10s %10s %10s %10s %10s \r\n');

fprintf(fileID,formatSpec2,'t','BV','Ct','qt','theta');

%formatSpec = strcat(formatSpec,'%10.3f %10.5f %10.3f %10.3f %10.8f');

formatSpec = strcat(formatSpec,' %.3E %.3E %.3E %.3E %.3E');

fprintf(fileID,strcat(formatSpec,'\r\n'),results_table.');

fclose(fileID);


end


end



function dCdt = DiffEq(t,conditions)

global day;

global exp;

global i;

global qt;


time=t;


j = exp(1,3);

Cinfluent = exp(1,4);

k = exp(1,5);

Cs = exp(1,6);
```

```
KF = exp(1,7);

n = exp(1,8);


Ct = conditions(1);   %ug L-1

qt(i) = conditions(2);   %ug L-1

Ct_mgL = Ct/1000;          %mg L-1

qt_mgg = qt(i)/(Cs*1000);    %mg g-1


%the rate equation we are using is

%dqt/dt = k' * Ct * (1-(qt/(Kf * Ce^(1/n))))^2

%please see our manuscript for derivation and further information


rate_ads = 1000*k*Ct_mgL*Cs*((1-(qt_mgg/(KF*(Ct_mgL^(1/n)))))^2); %calculate dq/dt
in ppb L-1 min-1

if conditions(1) <0

   conditions(1) = 0.00000001;   %Ct can never be negative, otherwise this seems to
slow down the simulation

   rate_ads=0;

end

rate_influx = j*Cinfluent; %calculate the rate of sorbate influx (continuous-flow
systems only)

rate_outflux = j*Ct; %calculate the rate of sorbate outflux (continuous-flow
systems only)

dCdt = [-rate_ads+rate_influx-rate_outflux;rate_ads]; %adjust the concentration of
aqueous sorbate and adsorbed sorbate, respectively


%finally we need to update qt(i) so that the next day's simulation begins

%with the appropriate amount of sorbate already attached.

qt(i)=qt(i)+rate_ads;


%print the variables out for debugging

"t is " + t + ", Ct is " + Ct + " ug L-1 and qt is " + qt(i) + "ug L-1, day " + day
+ ", i is " + i

end
```

6. References

(1) Lützenkirchen, J.; Preočanin, T.; Kovačević, D.; Tomišić, V.; Lövgren, L.; Kallay, N. Potentiometric Titrations as a Tool for Surface Charge Determination. *Croat. Chem. acta* **2012**, *85* (4), 391–417. https://doi.org/10.5562/cca2062.

(2) Salaün, P.; Planer-Friedrich, B.; van den Berg, C. M. G. Inorganic Arsenic Speciation in Water and Seawater by Anodic Stripping Voltammetry with a Gold Microelectrode. *Anal. Chim. Acta* **2007**, *585* (2), 312–322. https://doi.org/10.1016/j.aca.2006.12.048.

(3) Cheng, A.; Tyne, R.; Kwok, Y. T.; Rees, L.; Craig, L.; Lapinee, C.; D'Arcy, M.; Weiss, D. J.; Salaün, P. Investigating Arsenic Contents in Surface and Drinking Water by Voltammetry and the Method of Standard Additions. *J. Chem. Educ.* **2016**, acs.jchemed.6b00025. https://doi.org/10.1021/acs.jchemed.6b00025.

(4) Ayawei, N.; Ebelegi, A. N.; Wankasi, D. Modelling and Interpretation of Adsorption Isotherms. *J. Chem.* **2017**, *2017*. https://doi.org/10.1155/2017/3039817.

(5) Kosmulski, M. Isoelectric Points and Points of Zero Charge of Metal (Hydr)Oxides: 50 Years after Parks' Review. *Adv. Colloid Interface Sci.* **2016**, *238*, 1–61. https://doi.org/10.1016/j.cis.2016.10.005.

(6) Bullen, J. C.; Saleesongsom, S.; Weiss, D. J. A Revised Pseudo-Second Order Kinetic Model for Adsorption, Sensitive to Changes in Sorbate and Sorbent Concentrations. *ChemRxiv Prepr.* **2020**. https://doi.org/10.26434/chemrxiv.12008799.

(7) Huang, Y.; Farooq, M. U.; Lai, S.; Feng, X.; Sampranpiboon, P.; Wang, X.; Huang, W. Model Fitting of Sorption Kinetics Data: Misapplications Overlooked and Their Rectifications. *AIChE J.* **2018**, *64* (5), 1793–1805. https://doi.org/10.1002/aic.16051.

(8) Bullen, J. C. MATLAB Codes - A Kinetic Adsorption Model for Modelling Arsenic Treatment Plant (ATP) Lifetimes. 2020. https://doi.org/10.5281/zenodo.3690170.